

AD A953060

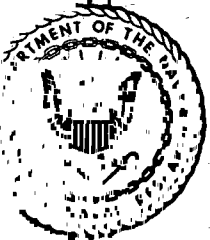
CHARACTERISTICS OF THE LIGHT WEIGHT HIGH-IMPACT SHOCK MACHINE

R. W. Conrad

Shock and Vibration Branch
Mechanics Division

APPROVED FOR PUBLIC RELEASE
DISTRIBUTION UNLIMITED

January 23, 1952



NAVAL RESEARCH LABORATORY

WASHINGTON, D.C.

RECEIVED
TECHNICAL
JAN 23 1952
NAVAL RESEARCH LABORATORY

ABSTRACT

A study was made of the light weight shock machine to determine its characteristics when operated according to standard shock-test specifications. Concentrated loads were secured to both the standard 4A and shelf mounting plates and subjected to hammer drops, from heights ranging between 1 and 5 ft, delivered to the back, edge, and top. Load weights varied from a minimum of 57 lb (instrumentation only) to a maximum of 389 lb, and comprised a welded-base assembly and sections of steel plates. These were bolted to the mounting plates by four 3/4-in-diameter bolts arranged in a rectangular pattern, and were spaced away from the plates by two-in. pedestals. Two directions of orientation were permitted by the rectangular bolt pattern on the 4A plate—with either the long bolting dimension vertical or the long bolting dimension horizontal. However, only one orientation was used with shelf-mounted loads.

Instrumentation comprised an accelerometer, a velocity meter, and a multi-frequency reed gage located on the load, and a second accelerometer mounted in a remote position on the mounting plates. Adaptors were employed for positioning the pickups to measure the shock motions in the direction of hammer impact. Output signals were recorded photographically as a function of time by a multichannel cathode-ray oscillograph, and simultaneously by a paralleled Mirragraph system.

Peak values of acceleration and velocity were measured on the load for the numerous variations in test parameters, and curves were prepared showing the relation of the peak values to the intensity of the hammer blow. It is shown that the peak velocities for a given test condition are approximately linearly related to the hammer-impact velocity. Peak accelerations evidenced a greater scatter of data and necessitated analysis in terms of averages. Values in the range of 500 g (1000-cps low-pass filter) were the maximum measured on the load as the result of a 5-ft hammer drop, and occurred during back blows to horizontally oriented loads on the 4A plate. Loads mounted on the shelf plate received the least severe shocks.

Both peak acceleration and velocity data showed small scatter for duplicate blows, if the blows were taken in succession or if the load was not disturbed between blows. However, if a test condition was repeated after intervening blows to other loads and arrangements, considerable variations of peak values often occurred.

PROBLEM STATUS

This is an interim report, work on this problem is continuing.

AUTHORIZATION

NRL Problem F03-38R
RDB Project NS 711-101

Manuscript received November 29, 1951

UNCLASSIFIED

CONTENTS

INTRODUCTION	1
DESCRIPTION OF LIGHT WEIGHT SHOCK MACHINE	2
METHODS OF TEST	4
Loads	4
Hammer Drops	8
Instrumentation	8
EXPERIMENTAL RESULTS	12
Acceleration Measurements	12
Load Acceleration	13
Mounting-Plate Acceleration	19
Load Velocity	22
Load Displacement	30
Reproducibility of Data	31
SUMMARY	32
CONCLUSIONS	33
ACKNOWLEDGMENTS	34
REFERENCES	34

APPROVED FOR PUBLIC RELEASE
DISTRIBUTION UNLIMITED

CHARACTERISTICS OF THE LIGHT WEIGHT HIGH-IMPACT SHOCK MACHINE

INTRODUCTION

Prior to the early stages of World War II, the principal causes of damage to shipboard equipment resulted from direct hits by enemy shells and torpedoes or from the firing of the ship's own guns. It was generally conceded that the only protection against enemy action which could be afforded equipment was to mount it as far as possible from the hull plating and to carry as much armor as was practical. Shortly after World War I, a ruggedization program was launched to increase the resistance to gun-blast damage for equipment which was required to be mounted in the general vicinity of gun turrets. The 250 Ft-Lb Shock Machine (1) was designed for this purpose and permitted laboratory evaluation and study of constructional weaknesses in equipment and the efficacy of design changes. Somewhat later, a combination machine, capable of subjecting equipments to rock and roll, shock, and vibration, was developed by the Radio Transmitter Section of the Laboratory (2).

During World War II, the problems of equipment protection increased enormously because of several factors. Development of noncontact bombs and influence mines which exploded below the water surface in the immediate vicinity of the ship caused appreciable damage of a general nature throughout the ship, without necessarily causing hull damage. Heavy equipment in engine-room compartments, which had been comparatively safe, became misaligned or inoperative because of casing or mount fractures. Under more severe shocks, this heavy equipment was completely dislodged and became a secondary missile itself. Lighter equipment which survived destruction, because of flexibility in its frame and mounts, nevertheless, often was rendered inoperative by excessive motion and interference between internal parts. Shock damage was most severe in spaces below the water level and decreased in intensity as the shock propagated through the ship's structure. The superstructure and above-deck spaces suffered the least from underwater explosions, but remained the most susceptible to blast and shell damage.

Increased reliance on complex electronic equipment further complicated the shock-protection program. Radar and sonar equipments were new devices which, because of their complexity and unique characteristics, were readily rendered inoperative or ineffective by combat conditions. The Navy was vitally interested in shock protection and ruggedization programs, and vigorously pursued them. To provide laboratories with testing facilities which could duplicate this new type of shock motion, a shock machine based on British design was built for the Navy by General Electric in 1940. Damage inflicted on equipment by this new shock machine reasonably duplicated that encountered by similar equipment in fleet service, and the machine was accepted as a valuable laboratory tool for studying the new shock problems and for improving the resistance to shock of numerous shipboard equipments. Since the machine could accommodate only light weight equipment, presently limited to 250 lb, the machine was designated as the

Light Weight High-Impact Shock Machine. At present there are about 30 light weight shock machines installed in manufacturers plants and government laboratories engaged to study the characteristics of shock and to improve the shock resistance of naval equipment.

A Medium Weight High-Impact Shock Machine was installed at the Engineering Experiment Station (3) in 1942, followed shortly by similar installations at larger manufacturers plants, and at NRL (4) in 1946. Plans for a heavy weight shock machine are still tentative. Numerous other types of shock machines also have been designed, each with a particular application or characteristic in mind. A partial list includes: The Taft-Pierce Shock Machine for Electronic Devices (5), A Medium Impact Variable Duration Shock Machine (AMC) (6), The 3 Ft-Lb Vibration Machine (7), and a Drop Table Shock Tester (8). Other Government laboratories have specialized devices for producing the types and magnitudes of shock of most interest to them; for example, the air guns at the Naval Ordnance Laboratory and the explosion pit at the David Taylor Model Basin. With this array of shock machines there is undoubtedly some duplication of performance characteristics by machines of different design, as well as differences in characteristics of machines of the same type.

Numerous modifications and additions have been incorporated in the light weight shock machine as the need for them became apparent during the normal use of the machine, or as discrepancies were noted between different machines. The major changes to date have been to incorporate hammers having spherical striking surfaces, to increase the lateral arm stiffness of the swinging hammer, to replace the original leaf springs by helical springs, and to standardize on an anvil travel of 1.5 inches to position stops. These modifications were made in the two NRL light weight shock machines in 1945. Tests (9) based on displacement records indicated that the machines with the modified characteristics were more uniform for blows delivered from the three directions, and for blows delivered by different machines.

The present investigation was intended to provide data on the shock motions delivered at the load position on the light weight shock machine, when operated under conditions governed by standard shock-test specifications (10, 11). Test runs were begun on the NRL machine No. 2 in October 1950 and completed in December.

DESCRIPTION OF THE LIGHT WEIGHT SHOCK MACHINE

In the interest of completeness, the salient constructional features of the light weight shock machine (Figure 1) will be summarized, although it is a familiar device to most persons who have been engaged in shock work. The machine comprises a welded frame of standard steel sections; two hammers, one dropping vertically, and the other swinging in a vertical arc; and an anvil plate which may be placed in either of two positions. The combination of two hammers and two anvil-plate positions permit blows to be delivered in each of three mutually perpendicular directions without remounting the test equipment. Each hammer weighs 400 lb and may be raised to a maximum height of 5 ft above its impact position, to deliver a maximum of 2000 ft-lb of energy at impact.

The anvil plate is a steel plate measuring 34 x 48 x 5/8 inches, reinforced across its back surface by I-beam stiffeners. Steel shock-pads are welded to the top and side edges, and at the center of the back face over the stiffeners at the points of hammer impact. For back and top blows the anvil plate is positioned across the main frame and rests on a pair of enclosed helical springs. It is constrained to a vertical position by a

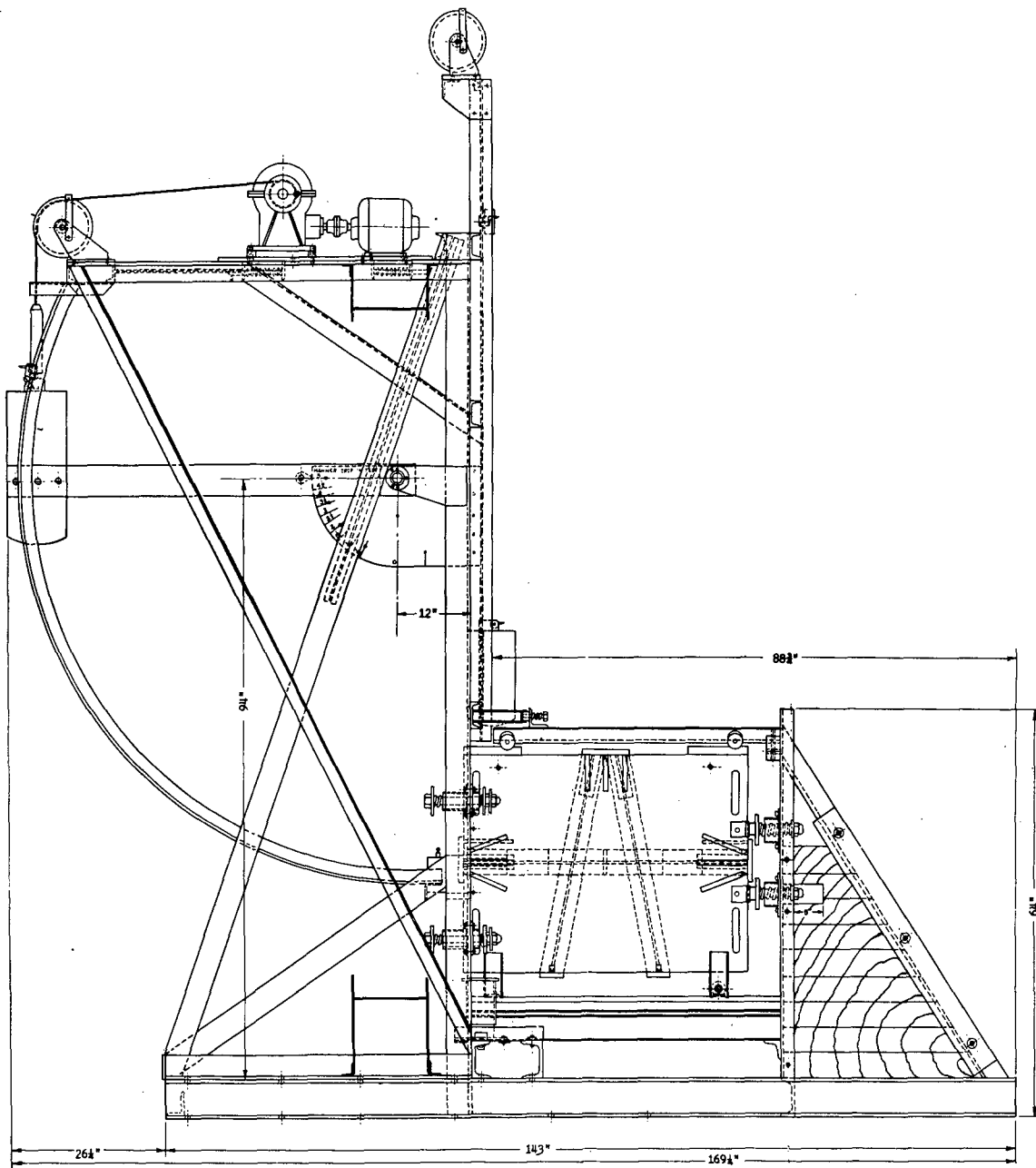


Figure 1 - Over-all view of light weight shock machine

set of springs and through bolts bearing against the main uprights. Washers and spacers prevent binding of the anvil plate during top blows. For edge blows, the anvil plate is rotated 90° around a vertical axis, and is supported by rollers bearing against steel tracks. It is positioned by a set of springs mounted on the forward support-brace edge. Edge blows are delivered by the swinging hammer against the rear anvil-plate edge. In each of the three directions of hammer impact the anvil-plate constraining springs are adjusted to permit 1.5 inches of forward motion against the springs before bottoming occurs against limit stops. Rebound springs for back and edge blows are also provided with limit stops, although these springs reach their solid height before the limits are reached. There are no rebound springs for top blows, the maximum spring extension being governed by a captive bolt. Forward springs are considerably softer than rebound springs, as Table 1 indicates.

TABLE 1
Stiffness of Anvil-Table
Positioning Springs

Direction of Blow	No. of Sets of Springs	Stiffness per Spring (lb/in.)	
		Forward	Rebound
Back	4	570	2000*
Edge	2	1260†	4900*
Top	2	475	--

*These springs are nonlinear and reach their solid height after about 0.4 inch of displacement.

†Two concentric springs in parallel

Back- and edge-blow positioning springs are precompressed by through bolts which adjust the maximum forward motion to 1.5 inches. Thus both the forward and rebound springs are under an initial static deflection when the anvil table is in its rest position, the rebound spring being compressed the least because of its greater stiffness. When a blow is struck, both springs act for about 0.1 inch of anvil travel after which the rebound spring reaches its free height, leaving the forward spring acting alone. A plot of the effective spring stiffness (per set of springs) seen by the anvil plate for a back blow is given by Figure 2. The change in slope as the rebound spring becomes free is quite pronounced, as is the nonlinearity in the rebound-spring loading curve. Similarly shaped curves are obtained for edge-blow springs.

METHODS OF TEST

Loads

It has been shown by repeated experiments and studies that the performance characteristics of the light weight shock machine are largely dependent on a number of factors: test-equipment weight and mounting dimensions, equipment-frame stiffness, plate-bolt tightness, and previous history of the anvil plate and mounting adaptor. These factors

influence the modes of vibration in the mounting plates, change natural frequencies, and alter their phase relationships with one another. The actual shock waveforms given two nearly identical pieces of equipment can therefore be quite different in character, although not necessarily of greatly different magnitude. It was the intent of this investigation, therefore, to obtain information on the light weight shock machine when operated under controlled test conditions which would closely approximate an "average" loading condition. Thus, the load dimensions were selected to correspond to equipment sizes most often received for shock testing, while operating techniques and bolt-tightening schedules duplicated those of actual shock tests.

To more nearly simulate the mounting conditions aboard ship, several standardized mounting plates have been devised. These are interposed between the anvil plate and the test equipment and provide a degree of flexibility and isolation to the shock motions which presumably duplicates the normal bulkhead stiffness. Two mounting plates are used predominately for specification shock tests: the 4A plate for bulkhead-mounted equipment (Figure 3), and the shelf mounting plate for platform-mounted equipment (Figure 4). The former derived its name from its figure number in shock-test specifications (11) and is a flat steel plate 27 x 34 x 1/2 inches, while the latter is a similar plate to which a reinforced shelf has been welded. Reinforced 4 in. x 13.8 lb car-building channels along the vertical edges space the mounting plates away from the anvil plate. Holes are drilled in the mounting plates as required to mount the test equipment centrally, the plate being discarded when the holes from previous tests become too numerous. Both the 4A and shelf plates were in new condition prior to this investigation, although the anvil plate had seen considerable service up to this time and was slightly distorted both as to its curvature and the shock-pad impact surfaces.

Detailed drawings of the load apparatus used during this investigation are given in Reference (12). The total weight capacity of the machine was covered by two separate load assemblies, the lighter covering the range up to 200 lb, and the heavier from 200 to 400 lb. A rugged welded frame comprised the base assembly in the light range (Figures 5 and 6) to which additional steel plates were bolted to increase the load weight in small increments of approximately 25 or 50 lb. In the heavier range the load consisted of two sections of solid steel plating (Figures 7, 8, and 9), one weighing approximately 200 lb and the other 125 lb. These sections could be used singly or in tandem to alter the load weight. Each load was drilled to accommodate the same rectangular mounting bolt pattern so that the load distribution on the mounting plate remained the same for all loads. Two-inch cylindrical pedestals spaced the load weight away from the mounting plate to prevent binding.

The rectangular mounting pattern permitted the load to be oriented in two directions and allowed the effects of load distribution to be studied. Two positions, one with the

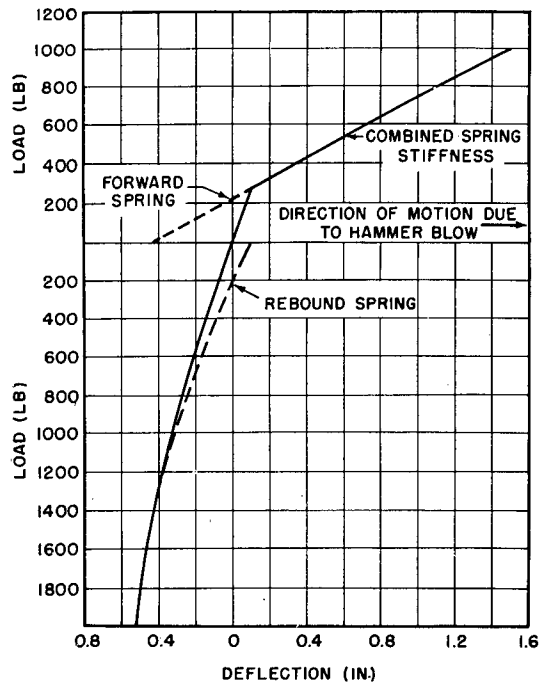


Figure 2 - Typical spring-stiffness curves for anvil-plate positioning springs, back blow

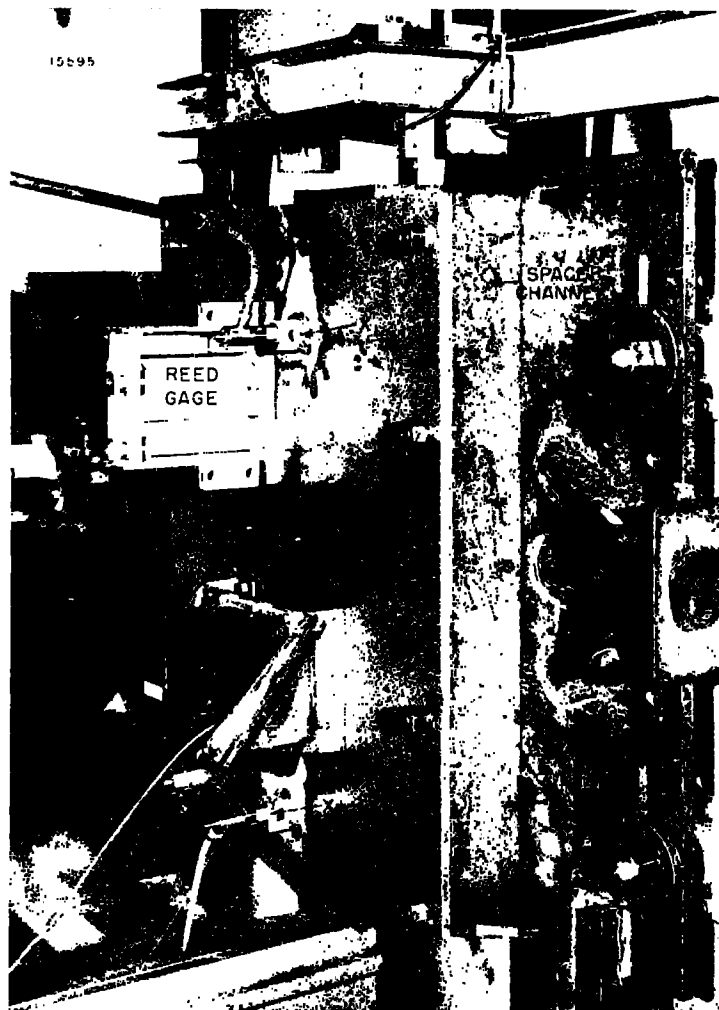


Figure 3 - Experimental setup for Run 0 back blow, 57-lb total load on 4A plate

long axis of the load vertical and one with it horizontal, were tested on the 4A mounting plate, whereas only one orientation was used with the shelf mounting plate. In the latter case the long axis was horizontal and parallel to the anvil plate. Run numbers were assigned each condition of test for ready identification. Back, edge, and top blows delivered to a particular loading arrangement were considered as belonging to the same run. Test conditions are summarized by Table 2. Runs 0 and 11 correspond to nominal no-load runs, i.e., the load comprised only the measuring instruments and their mounting adaptors bolted directly to the mounting plates. Runs 0 through 10 were made on the 4A plate, odd-numbered runs having the long axis of the load vertical and even-numbered runs with it horizontal. Thus Runs 1 and 2, 3 and 4, etc., are conjugate pairs whose test conditions differed only in load orientation. Measurements made on the shelf mounting plate were designated as Runs 11 through 16, and used the same loads as were used on the 4A plate. Photographs of several loading arrangements are shown in Figures 3 through 9.

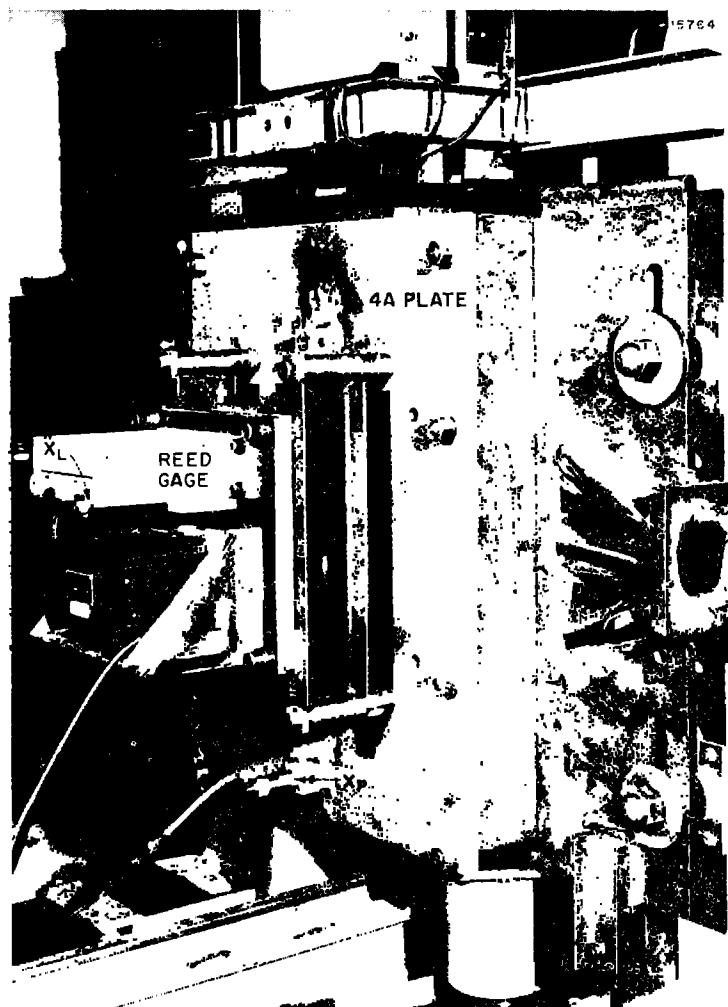


Figure 5 - Experimental setup for Run 3 back blow,
145-lb load vertically oriented on 4A plate

Hammer Drops

Each of the runs listed in Table 2 was further divided into blows delivered from the back, edge, and top, and for hammer-drop heights of 1, 2, 3, 4, and 5 ft. Thus all combinations of the machine parameters were investigated for each of the run conditions. Numerous runs were repeated to ascertain the repeatability of shock motions, or to further investigate various aspects of the performance of the machine.

Instrumentation

The principal objective of this investigation was to obtain information regarding the magnitudes and characteristics of the load-shock motions for the various conditions of load weight, height of drop, and direction of blow. In order to determine the salient

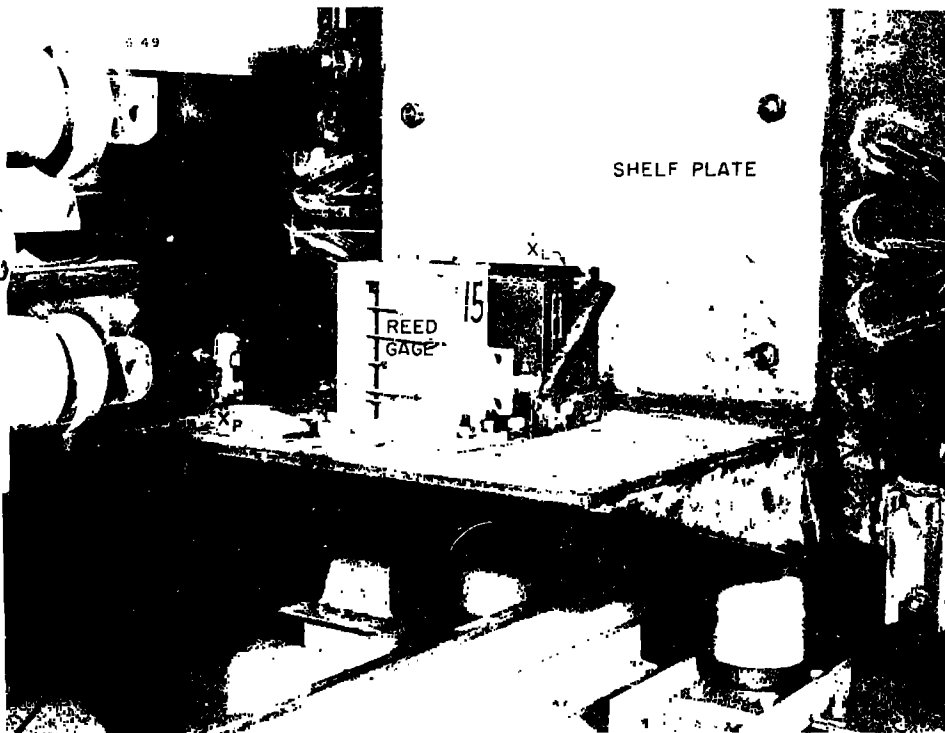


Figure 4 - Experimental setup for Run 11 top blow, 57-lb load on shelf plate

TABLE 2
Summary of Test Conditions Corresponding to Run Numbers

Load (lb)	4A Plate		Shelf Mounting Plate
	Load Axis Vertical	Load Axis Horizontal	
57*	0		11
121	1	2	12
145	3	4	13
192	5	6	14
261	7	8†	15
389	9	10	16

*Total weight of instruments and their mounting adaptors

†Run 8 was inadvertently omitted from the experimental agenda.

features of shock motion, measurements were made of velocity and acceleration as a function of time, and of the shock spectra as indicated by a multifrequency reed gage. These instruments were bolted directly to the load assembly and oriented to measure the shock motions in the direction of the hammer impact. A second accelerometer was maintained in a fixed position on each mounting plate, and provided an indication of the magnitude of shock motions at these specific locations.

With the possible exception of the reed gages, the instruments were standard types whose characteristics and limitations are well known, and which have proven satisfactory for shock measurements. Instrument locations and details of their mounting adaptors may be seen in Figures 3 through 9. Westinghouse quartz-crystal accelerometers (designated as \ddot{x}_L and \ddot{x}_P in Figures 3 through 9) were used at both the load and mounting-plate locations, despite their low output voltage as compared to other types, because they were the most rugged mechanically. Notwithstanding their inherent

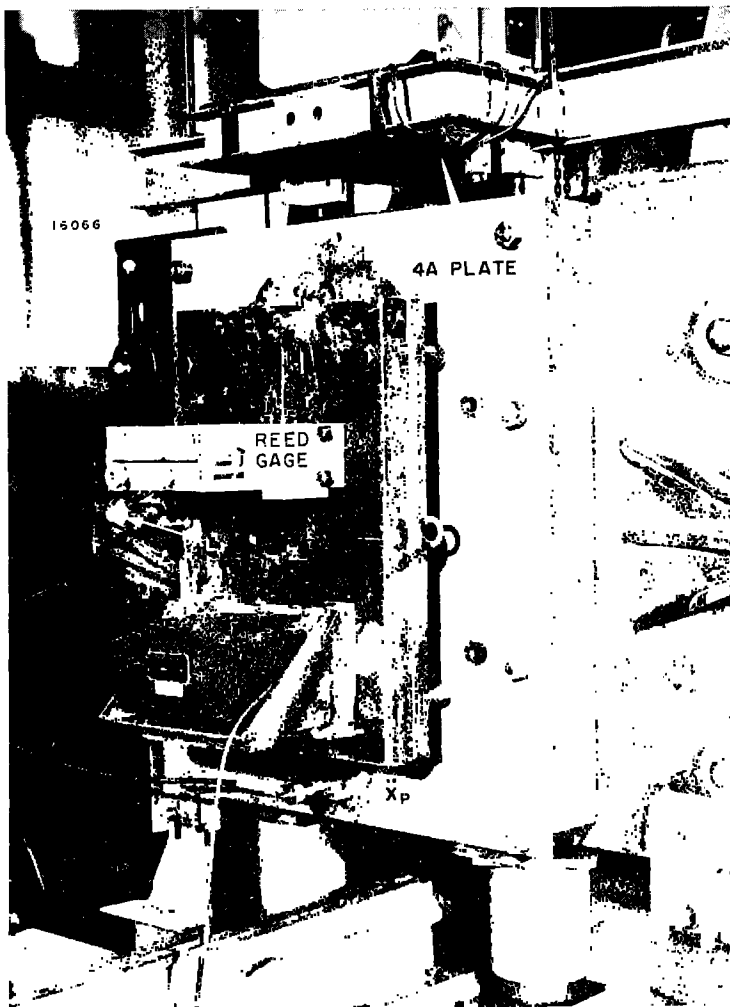


Figure 7 - Experimental setup for Run 9 Back blow,
389-lb load vertically oriented on 4A plate

sturdiness, the crystals became fractured as a result of the numerous blows, and a constant check of their condition was necessary. Additional precautions were observed to insure satisfactory results by employing a graphite impregnated connecting cable to minimize cable microphonics, and by supporting the cable away from the anvil plate in such a manner as to reduce bending and whipping during the blow. Standard 300-, 1000-, and 5000-cps low-pass filters, incorporated in the accelerometer preamplifiers, limited the upper frequency response of the acceleration signals by removing accelerometer resonances and the higher frequency acceleration components which are of little importance, i.e., have little damaging value, yet predominate in the unfiltered records. The filtered output signals were displayed simultaneously on a multichannel cathode-ray oscillograph and recorded photographically by a moving-film camera (Figures 10 and 11). Sufficient recording channels were available to permit recording each accelerometer signal on two channels at the same time, using different sets of filters. Thus, the 1000-cps filtered record was recorded for every blow, while the paralleled channel alternated between a 300-, and a 5000-cps filter.

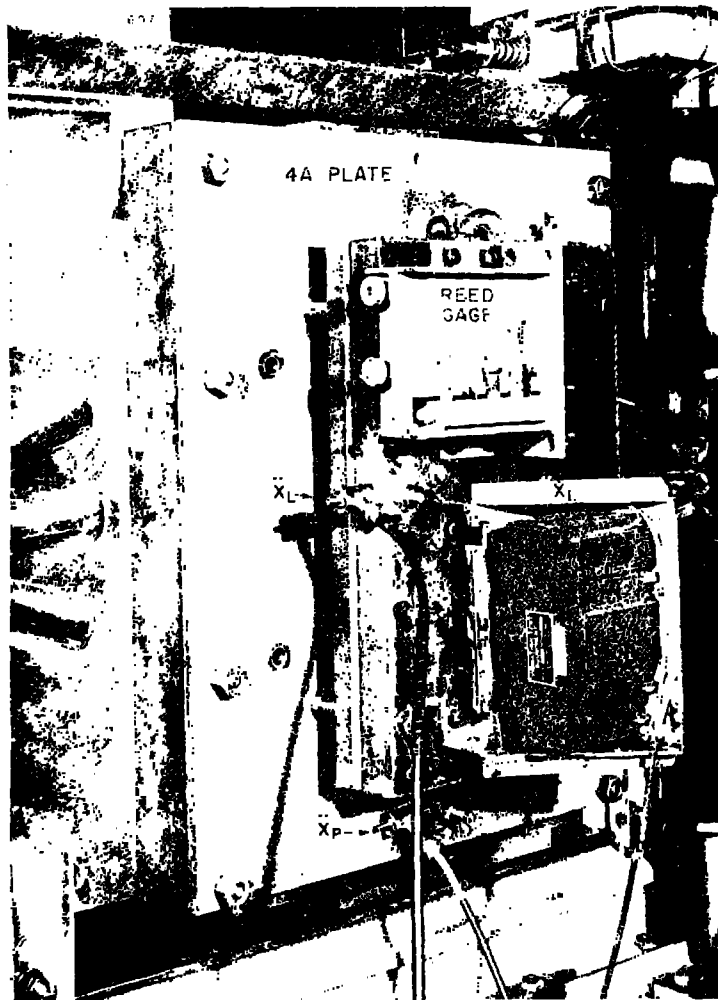


Figure 8 - Experimental setup for Run 9 edge blow, 389-lb load vertically oriented on 4A plate

The velocity meter was an MB Type 200 which had previously been modified to reduce its natural frequency from 6 cps to 2.5 cps. This instrument has a nominal displacement capacity of 3 inches, and was adequate to accommodate the maximum anvil-plate travel in any direction. Output signals were shunted by a 10-ohm damping resistor, and recorded photographically, unfiltered, on the fifth channel of the cathode-ray oscillograph.

Typical cathode-ray oscillograph test records (Figures 10 and 11) demonstrate the type of waveforms encountered on the light weight shock machine under the conditions stated.

The displacement of the time axis exhibited by the plate-acceleration traces results from the physical arrangement of the cathode-ray tubes, and does not reflect a delay between the corresponding signals.

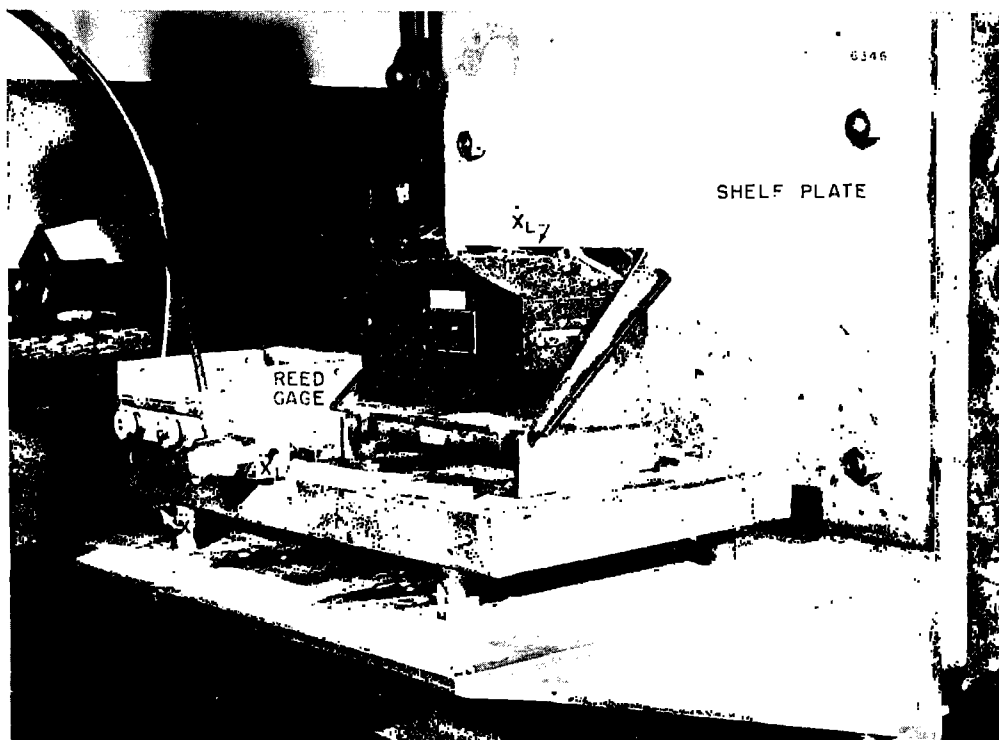


Figure 9 - Experimental setup for Run 15 back blow, 261-lb load on shelf plate

Electrical output signals from the test instruments were also recorded simultaneously by a Mirragraph assembly to facilitate analysis of these records by analog systems. These data and reed-gage shock spectra will be covered by a separate report.

EXPERIMENTAL RESULTS

As is apparent from the typical test records, the shock waveforms, produced by the light weight shock machine, exhibit the same general characteristics for different heights of hammer blow delivered to a particular load arrangement, but greatly modify their characteristics with changes in direction of blow, load weight, load orientation, and mounting plates. Previous history of the anvil and mounting plates also affect the shock waveforms, but to a much lesser extent, by their influence on the plate stiffnesses and vibratory modes. For these reasons, a theoretical treatment was not attempted. Dependence of the shock waveforms and their peak magnitudes on so many variables increases the difficulty of correlating these data with the test parameters. Consequently, the following experimental data is presented with little attempt being made to relate the values obtained in the different parametric groups.

Acceleration Measurements

Positions of the load and mounting-plate accelerometers may be seen in the photographs of load arrangements (Figures 3 through 9). The choice of these locations was

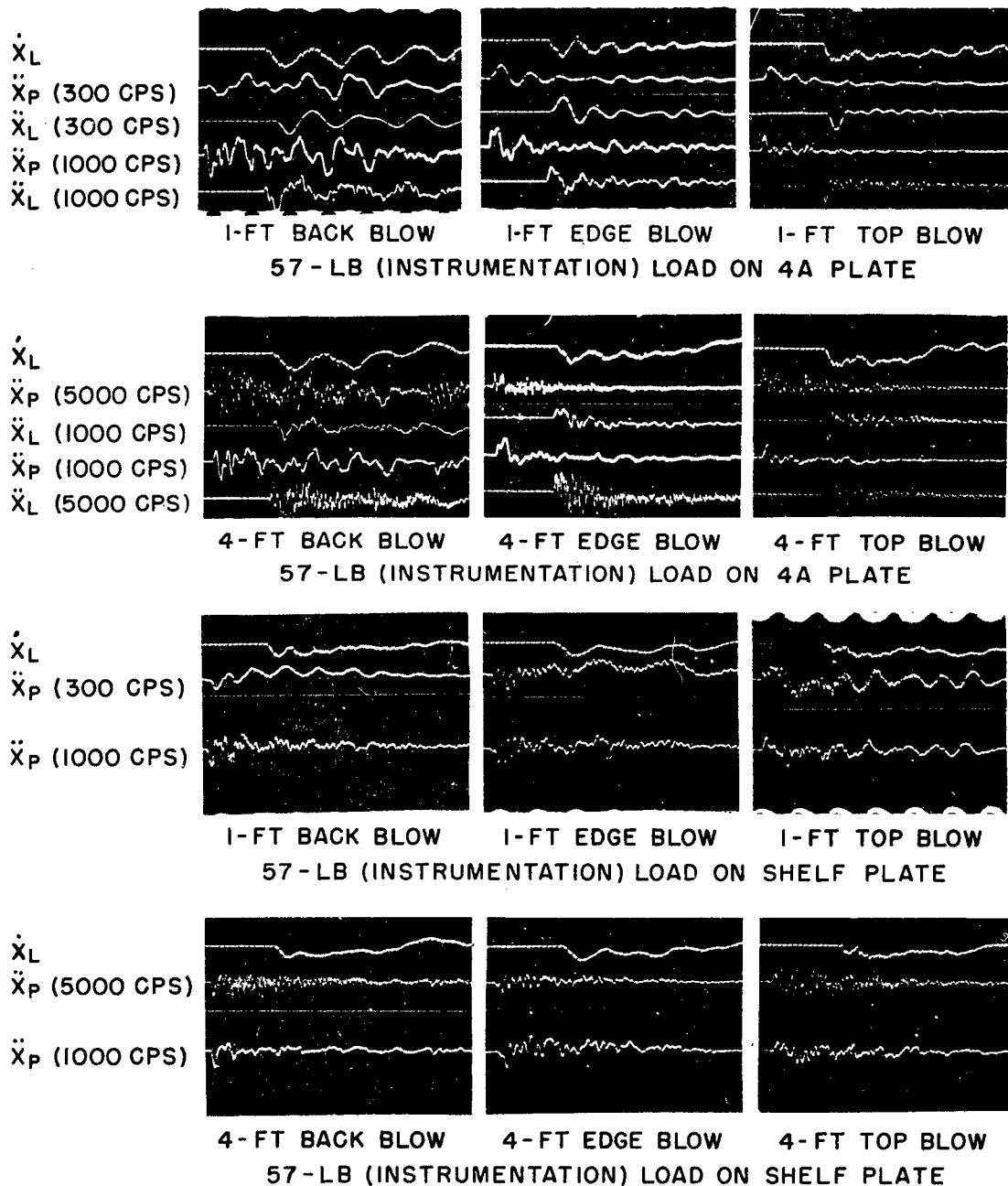
dictated by space availability and expediency in altering the orientation of the accelerometer to comply with the direction of hammer impact. The load accelerometer position was not critical as the load was inflexible enough to be considered a rigid body. On the other hand, acceleration waveforms and magnitudes on the mounting plates are dependent on the location of measurement. Positions were chosen at the bottom center of the 4A plate and at the center of an outboard stiffener of the shelf plate.

Although special precautions were taken to minimize errors from cable microphonics, instances were noted where the charge generated by the cable resulted in a noticeable zero shift in the acceleration records. This was especially true for the 300-cps filter records where additional amplifier gain was required to compensate for the reduced signal level in the frequency range below 300 cps. It is doubtful, however, that there was sufficient anvil-plate motion up to the time of the first acceleration peak, usually not more than 2 milliseconds after impact, to cause any serious shift up to that time. However, when the shift did occur, it was noticeable shortly after the first half cycle. Fractured crystals in the accelerometers also contributed to questionable records and required that repeat blows be made. Except in extreme cases when the crystals become pulverized, and intermittent shorts existed, it was virtually impossible to determine exactly when the pickup became deranged, since the waveforms and peak amplitudes closely resemble those obtained with an accelerometer known to be in good condition. In fact, a repeat blow, made after intervening blows from other directions, showed a much greater difference in acceleration than resulted from fractured crystals. For these reasons, the accelerometer records selected for analysis are assumed to be valid for the first few milliseconds, irrespective of zero shift and the possibility of fractured crystals.

The acceleration traces for both the load and mounting plates are shown on the typical test records (Figures 10 and 11). In general, the peak acceleration occurs shortly after impact, followed by irregular perturbations resulting from the random combination of the numerous vibratory modes excited by the hammer impact. The peaks occur on approximate half sine pulses for the 300- and 1000-cps filter records and on superimposed high-frequency vibrations for 5000-cps filter records. Durations of the pulses (1000-cps filter) average about 2 milliseconds on the mounting plates and about twice that on the load. Characteristics of the pulse vary with direction of blow and the mounting plate in use, but the duration remains essentially constant. The magnitude and frequencies of the acceleration which follows the peak are greatly influenced by a large number of factors such as bolt tightness, minor changes of stiffness, mass distribution, and energy dissipation. Slight variations in any of these factors produce large changes in the waveform after the first pulse. Records taken using the 5000-cps filter are worst in this respect, since the higher frequencies passed by this filter predominate and obscured even the most pronounced rigid-body motions. On the other hand, 300-cps filter records are devoid of all but the lowest frequencies, which in this case are those frequencies which dominate the velocity records. However, 300-cps filtration prevents proper reproduction of important components of the initial pulse which has a period comparable to the cutoff period. The 1000-cps filter was therefore selected as best for this type of recording. It represents a compromise by removing a large part of the high-frequency hash without eliminating frequencies which are distinguishable in velocity records.

Load Acceleration

A summary of the peak accelerations measured on the load by the 300-, 1000-, and 5000-cps filters for each of the conditions of test is given in Table 3. Figures given are the averages of individual readings when duplicate blows were delivered, with average



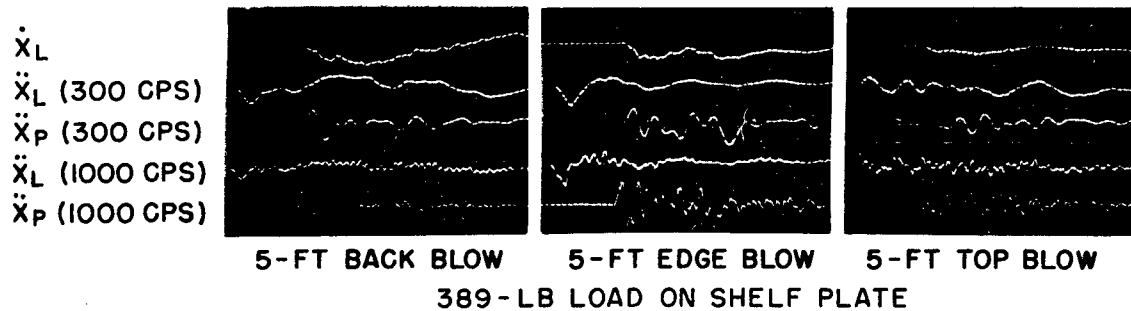
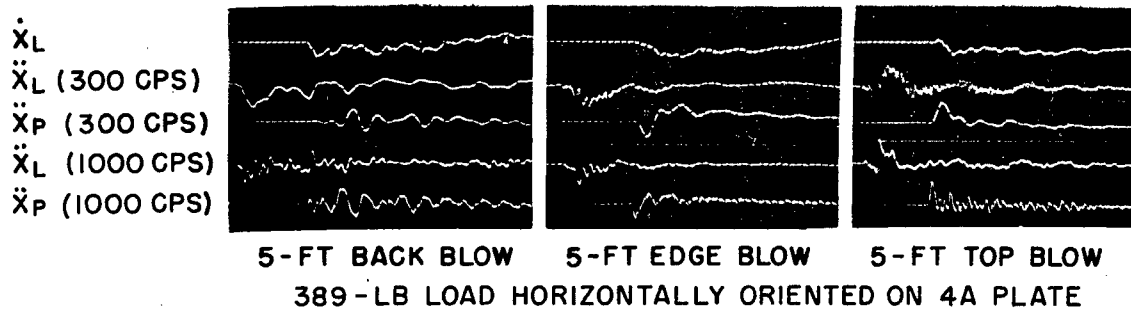
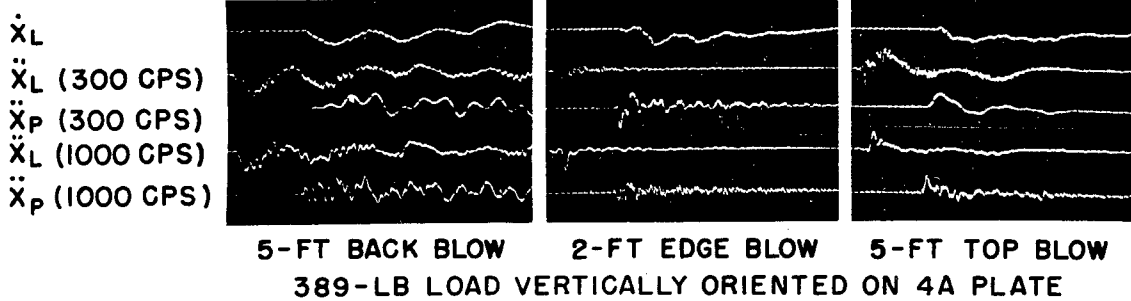
\dot{X}_L - LOAD VELOCITY

\ddot{X}_L - LOAD ACCELERATION
 \ddot{X}_P - PLATE ACCELERATION

} FILTER CUTOFF FREQUENCY
 GIVEN IN PARENTHESES

BLANKING FREQUENCY - 1000 CPS

Figure 10 - Typical test records



\dot{X}_L - LOAD VELOCITY
 \ddot{X}_L - LOAD ACCELERATION
 \ddot{X}_P - PLATE ACCELERATION

} FILTER CUTOFF FREQUENCY
 GIVEN IN PARENTHESES

BLANKING FREQUENCY - 1000 CPS

Figure 11 - Typical test records

TABLE 3
Peak Load Acceleration

Load (lb)	Ht Drop (ft)	4A Plate - Long Axis Vertical									4A Plate - Long Axis Horizontal									Shelf Mounting Plate											
		Direction of Blow									Direction of Blow									Direction of Blow											
		Back			Edge			Top			Back			Edge			Top			Back			Edge			Top					
		Avg Accel (g)	Avg Dev (%)	Max Dev (%)	Avg Accel (g)	Avg Dev (%)	Max Dev (%)	Avg Accel (g)	Avg Dev (%)	Max Dev (%)	Avg Accel (g)	Avg Dev (%)	Max Dev (%)	Avg Accel (g)	Avg Dev (%)	Max Dev (%)	Avg Accel (g)	Avg Dev (%)	Max Dev (%)	Avg Accel (g)	Avg Dev (%)	Max Dev (%)	Avg Accel (g)	Avg Dev (%)	Max Dev (%)	Avg Accel (g)	Avg Dev (%)	Max Dev (%)			
300-cps Filter																															
57	1	168	8	-	97	-	-	72	8	11																					
	3	199	12	23	204	-	-	133	10	27																					
	5	181	-	-	265	-	-	161	14	22																					
121	1	83	-	-	58	-	-	97	-	-	106	-	-	87	-	-	57	-	-	60	-	-	35	-	-	25	-	-			
	3	131	-	-	174	5	-	45	20	-	184	-	-	131	-	-	98	-	-	82	11	-	65	-	-	51	-	-			
	5	153	-	-	217	-	-	56	-	-	327	-	-	214	-	-	97	-	-	98	15	-	89	-	-	59	-	-			
145	1	-	-	-	64	3	-	67	0	-	144	-	-	76	50	-	42	29	-	53	-	-	45	-	-	10	-	-			
	3	-	-	-	111	-	-	98	-	-	274	-	-	140	19	-	64	17	-	70	-	-	69	-	-	41	-	-			
	5	-	-	-	146	-	-	125	-	-	242	-	-	198	17	-	62	21	-	93	-	-	80	-	-	57	-	-			
192	1	89	-	-	85	-	-	63	-	-	113	-	-	85	15	-	39	5	8	46	11	-	37	8	11	27	15	22			
	3	134	-	-	132	-	-	86	-	-	168	16	-	129	40	-	72	11	15	62	24	-	56	9	16	46	2	4			
	5	177	-	-	101	-	-	91	-	-	214	2	-	216	18	-	98	26	-	75	28	-	74	4	8	56	4	4			
261	1	122	-	-	69	-	-	39	-	-										37	24	-	40	5	5	31	0	-			
	3	126	-	-	127	-	-	-	-	-										62	11	18	72	8	-	61	7	-			
	5	197	-	-	193	-	-	89	-	-										89	9	-	92	14	-	73	4	-			
389	1	60	-	-	70	-	-	33	-	-	78	-	-	78	-	-	34	-	-	28	0	-	35	3	3	27	4	-			
	3	52	-	-	132	-	-	70	-	-	138	-	-	181	-	-	54	-	-	52	6	-	64	5	6	59	7	-			
	5	182	-	-	284	-	-	84	-	-	207	-	-	198	-	-	77	-	-	77	11	-	89	6	8	47	36	-			
1000-cps Filter																															
57	1	249	9	-	161	-	-	148	19	29																					
	2	395	7	11	256	-	-	200	22	32																					
	3	403	6	9	298	-	-	260	13	38																					
	4	481	6	-	275	-	-	274	26	33																					
	5	470	-	-	378	-	-	338	15	33																					
121	1	96	-	-	75	0	0	168	1	1	198	-	-	194	-	-	77	-	-	73	-	-	52	-	-	38	-	-			
	2	165	-	-	231	4	4	202	0	0	301	-	-	242	-	-	105	-	-	102	3	5	80	-	-	55	-	-			
	3	166	-	-	246	5	5	78	9	-	353	-	-	246	-	-	130	-	-	118	2	-	81	-	-	82	-	-			
	4	242	-	-	302	-	-	177	-	-	429	-	-	303	0	-	165	-	-	133	2	-	85	-	-	76	-	-			
	5	218	-	-	381	-	-	85	-	-	512	-	-	367	-	-	146	-	-	138	17	-	122	-	-	75	-	-			
145	1	-	-	-	83	2	-	126	5	-	254	-	-	156	4	4	66	2	2	62	-	-	60	-	-	44	-	-			
	2	131	-	-	135	-	-	166	-	-	315	-	-	194	6	-	108	22	-	86	-	-	82	-	-	64	-	-			
	3	-	-	-	142	-	-	173	-	-	391	-	-	260	7	-	124	3	-	83	-	-	96	-	-	53	-	-			
	4	153	-	-	201	-	-	201	-	-	476	-	-	275	1	-	126	12	-	82	-	-	97	-	-	75	-	-			
	5	-	-	-	184	-	-	201	-	-	537	-	-	332	4	-	148	5	-	121	-	-	93	-	-	102	-	-			
192	1	106	-	-	112	-	-	126	-	-	197	-	-	108	6	-	67	13	19	55	11	-	55	0	1	53	8	11			
	2	163	-	-	163	2	-	136	-	-	256	7	-	193	15	-	85	13	-	77	4	-	68	18	26	70	2	2			
	3	183	-	-	184	-	-	159	-	-	324	3	-	203	30	-	103	4	5	78	20	-	72	11	11	83	2	4			
	4	212	-	-	206	-	-	185	-	-	396	7	-	332	-	-	117	7	-	96	2	-	79	16	20	84	11	17			
	5	230	-	-	210	-	-	174	-	-	406	4	-	326	12	-	123	9	-	100	10	-	97	12	18	96	3	4			
261	1	102	-	-	68	-	-	39	-	-										53	28	-	55	2	-	55	15	-			
	2	138	-	-	139	-	-	65	-	-										74	32	-	75	8	-	82	19	-			
	3	160	-	-	194	-	-	17	-	-										83	21	31	97	6	-	108	18	-			
	4	210	-	-	202	-	-	77	-	-										103	15	-	102	7	11	130	15	23			
	5	206	-	-	218	-	-	114	-	-										119	19	-	121	12	-	141	16	-			
389	1	60	-	-	99	-	-	41	-	-	133	-	-	106	-	-	42	-	-	38	5	-	39	3	5	56	9	-			
	2	97	-	-	226	-	-	62	-	-	181	-	-	165	-	-	73	-	-	55	11	-	63	5	8	76	8	16			
	3	97	-	-	252	-	-	98	-	-	264	-	-	231	-	-	80	-	-	69	9	-	78	5	6	87	16	-			
	4	106	-	-	254	-	-	123	-	-	258	-	-	290	-	-	101	-	-	73	12	-	97	4	9	86	21	-			
	5	189	-	-	368	-	-	135	-	-	322	-	-	327	-	-	119	-	-	81	17	-	119	3	6	94	23	-			
5000-cps Filter																															
57	2	401	26	39	319	-	-	362	14	-																					
	4	582	33	-	444	-	-	469	23	-																					
121	2	215	-	-	312	-	-	245	-	-	391	-	-	426	-	-	219	-	-	178	7	-	103	-	-	145	-	-			
	4	765	-	-	475	-	-	283	-	-	583	-	-	367	7	-	391	-	-	212	27	-	215	-	-	167	-	-			
145	2	225	-	-	284	-	-	221	-	-	423	-	-	362	25	-	188	16	-	166	-	-	151	-	-	98	-	-			
	4	284	-	-	451	-	-	258	-	-	635	-	-	389	21	-	187	6	-	233	-	-	212	-	-	137	-	-			
192	2	314	-	-	187	6	-	243	-	-	338	11	-	267	15	-	157	11	-	124	14	-	130	12	19	134	2	4			
	4	454	-	-	346	-	-	310	-	-	488	12	-	397	-	-	192	10	-	187	0	-	178	11	22	184	7	10			
261	2	612	-	-	210	-	-	132	-	-										192	21	-	190	18	-	216	28	-			
	4	406	-	-	302	-	-	224	-	-										247	23	-	254	3	4	367	17	26			
389	2	266	-	-	387	-	-	97	-	-	580	-	-	272	-	-	177	-	-	155	0	-	131	9	14	184	16	33			
	4	429	-	-	367	-	-	182	-	-	547	-	-	412	-	-	204	-	-	198	1	-	191	12	15	286	7				

and maximum deviations from these values expressed in percent. Many of these averages represent readings taken over an extended period of time with anvil position changes and different load arrangements intervening. It is probable that the major variations are changes in the higher-frequency components of the shock motions. Plots of the peak load accelerations (1000-cps filter) are shown as the upper curves of Figures 12 through 20. As can be seen, the data does not lend itself well to drawing smooth curves because of the large scatter. Rather than attempt an estimate of both the shape and position of average curves, broken line graphs were employed so that the points associated with each curve are clearly indicated. The hammer-impact velocity was selected as the independent variable and resulted in curves which tended toward straight lines if point scatter were omitted.

Table 4 was prepared to assist in studying the trends in peak load accelerations and the effects of varying the machine parameters. This tabulation was constructed from the peak accelerations for a single condition, weighted with respect to hammer-impact velocity, and then averaged. Unity was assigned to the largest value so obtained, the remainder being compared on a per-unit basis. These values are subject to considerable variations, as can be seen from Table 3, and are presented to establish comparative acceleration levels for the different directions of blow and different methods of mounting.

TABLE 4
Comparison of Peak Load Accelerations
(1000-cps Low-Pass Filtration)

Load (lb)	4A Plate - Long Axis Vertical			4A Plate - Long Axis Horizontal			Shelf-Mounting Plate		
	Direction of Blow			Direction of Blow			Direction of Blow		
	Back	Edge	Top	Back	Edge	Top	Back	Edge	Top
121	0.44	0.67	0.41	0.89	0.70	0.32	0.29	0.21	0.17
145	0.39	0.37	0.45	1.00	0.62	0.29	0.22	0.22	0.17
192	0.45	0.45	0.41	0.80	0.57	0.26	0.21	0.19	0.20
261	0.41	0.41	0.18	-	-	-	0.22	0.23	0.25
389	0.27	0.59	0.22	0.61	0.55	0.20	0.16	0.19	0.21
Avg	0.39	0.50	0.33	0.83	0.61	0.27	0.22	0.21	0.20
Group Avg	0.41			0.57			0.21		

Loads mounted in both directions on the 4A plate and on the shelf plate showed a slight decrease in peak acceleration as the load was increased through the range from 121 to 389 lb. Most decreases were small, especially for shelf-plate loads, and somewhat erratic. Although the load weight was varied over more than a 3 to 1 ratio, this change represented only about a 40-percent change in total weight of the anvil-plate assembly. This is roughly of the same magnitude as the decrease in peak load acceleration.

There was comparatively little difference in the severity of blows with respect to direction of hammer impact for loads vertically mounted on the 4A plate, or for

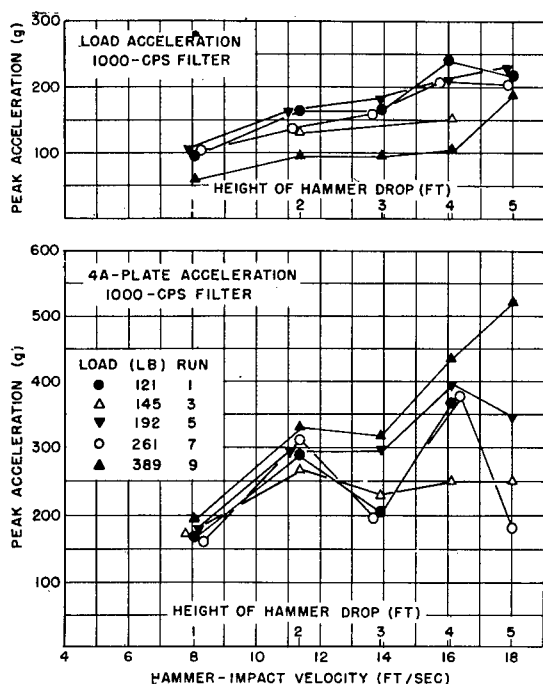


Figure 12 - Peak load and 4A-plate acceleration for back blows, load axis vertical

loads mounted on the shelf plate. The difference was more pronounced when the loads were oriented horizontally on the 4A plate—back blows became the most severe, and top blows the least. Comparative levels between the three methods of load attachment indicate that peak accelerations are roughly equivalent on the load, irrespective of the orientation of the load, for edge or top blows, but that back blows are considerably more severe when the loads are horizontally oriented than when they are vertically oriented. These results are reasonable since the 4A-plate stiffness in an edgewise direction is little affected by load orientation for either edge or top blows but increases in stiffness for back blows as the points of attachment are moved out toward the spacer channels. A horizontally positioned load would, therefore, be expected to receive larger peak accelerations. Acceleration levels on shelf-mounted loads are much smaller than those of equivalent conditions on the 4A plate.

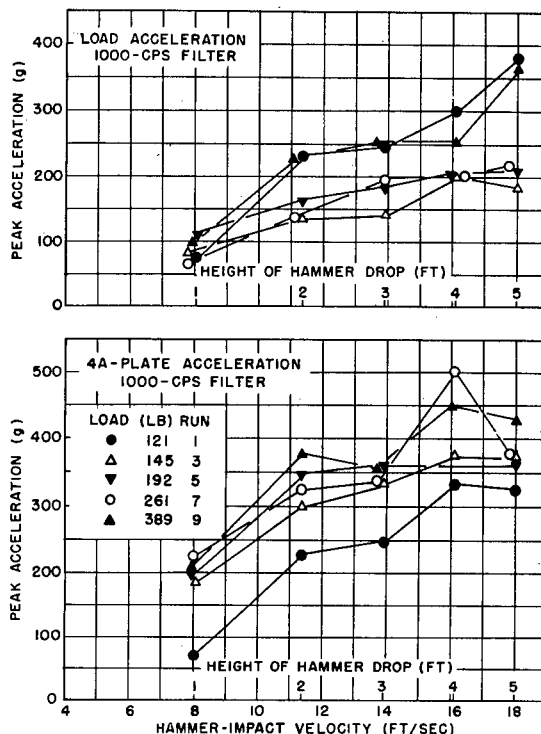


Figure 13 - Peak load and 4A-plate acceleration for edge blows, load axis vertical

Peak-acceleration magnitudes (1000-cps filter) caused by 5-ft hammer drops reached 537 g during a back blow, 4A-plate load horizontal; between 367 and 381 g during edge blows, 4A-plate loads in either position; between 201 and 230 g for back and top blows, 4A-plate load vertical; and between 122 and 148 g for all shelf-mounted loads and a top blow with 4A-plate load vertical. These figures represent the maximum recorded for each condition and did not necessarily occur for the lightest load.

Figure 21 is a plot of peak accelerations obtained on both the 4A plate and shelf mounting plate for the no-load runs. These data are not included with values obtained with concentrated loads, because the total weight of 57 lb was distributed over a large area of the mounting plates (Figure 3), and presented an entirely different loading on the plates. Both accelerometer positions experienced nearly equivalent peak accelerations on the 4A plate, since the load did not tend to bind the 4A plate appreciably. Back

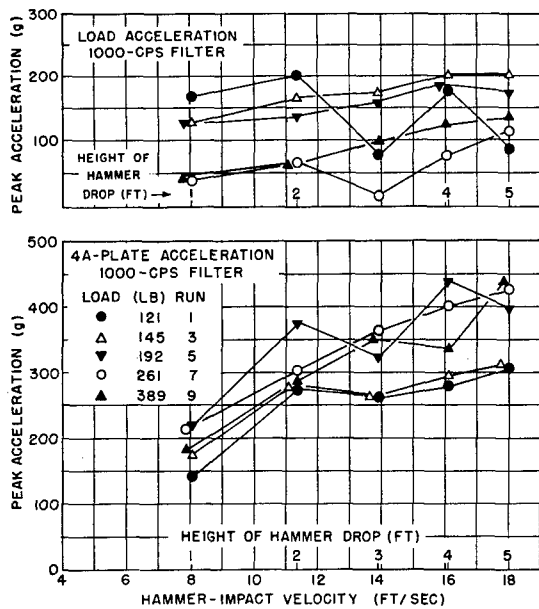


Figure 14 - Peak load and 4A-plate acceleration for top blows, load axis vertical

blows were considerably more severe than either edge or top blows, the latter being comparable. Peak acceleration on the shelf plate for the no-load runs were less than for corresponding directions of blows on the 4A plate, with a wide divergence between directions of blows. The levels of peak acceleration under these conditions are slightly greater than for rigid loads on the 4A plate, and roughly comparable on the shelf mounting plate.

Mounting-Plate Acceleration

The peak accelerations measured directly on the mounting plates are listed in Table 5. As was mentioned previously, the figures given in this table are peculiar to the accelerometer locations chosen and will differ for other locations, particularly as the position is moved closer to the spacer channels. Values given are the average peak acceleration where more than one blow was delivered, with average and maximum deviations expressed in percent. Table 6 was prepared, as before, to allow comparisons to be made of the individual test conditions. Although the peak accelerations measured on the 4A and shelf plates are compared on the same basis, they are not directly comparable because of their different locations. They were in equivalent positions with respect to the load, however.

The general trends in plate acceleration followed those evidenced by the load, except that the plate acceleration shows no tendency to decrease in magnitude with an increase in load. Horizontally mounted loads on the 4A plate yielded the largest plate accelerations because of the load's binding effect on the plate; shelf-plate accelerations were

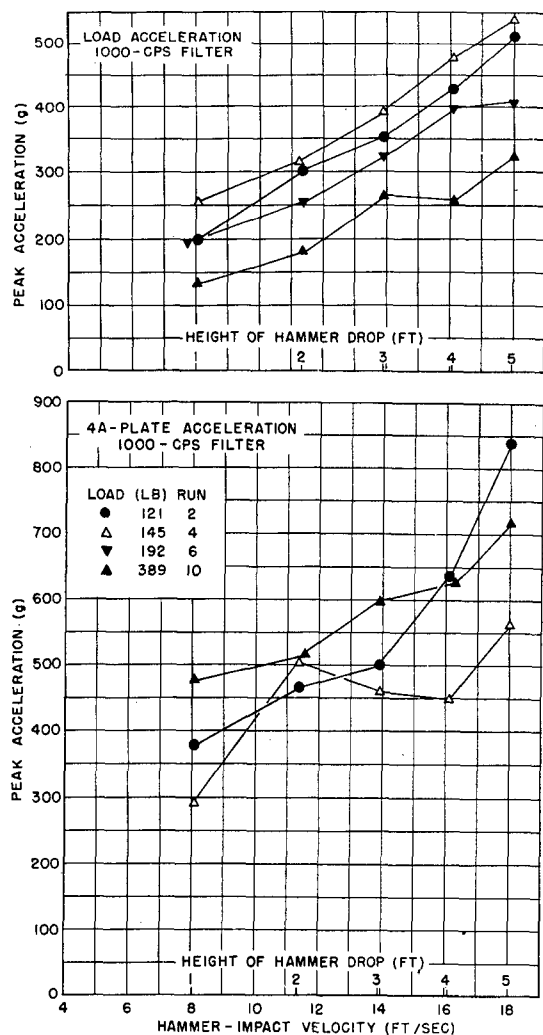


Figure 15 - Peakload and 4A-plate acceleration for back blows, load axis horizontal

Load (lb)	Ht (ft)	4A plate - Long Axis Vertical	4A plate - Long Axis Horizontal	Shelf-Mounting Plate	Direction of Blow			Direction of Blow		
					Back	Edge	Top	Back	Edge	Top
					Avg Accel	Avg Accel	Avg Accel	Avg Accel	Avg Accel	Avg Accel
					Drop	Drop	Drop	Drop	Drop	Drop
					Max	Max	Max	Max	Max	Max
					(g) (%)	(g) (%)	(g) (%)	(g) (%)	(g) (%)	(g) (%)
					Dev	Dev	Dev	Dev	Dev	Dev
					Max	Max	Max	Max	Max	Max
					Avg Accel	Avg Accel	Avg Accel	Avg Accel	Avg Accel	Avg Accel
					Drop	Drop	Drop	Drop	Drop	Drop
					Max	Max	Max	Max	Max	Max
					(g) (%)	(g) (%)	(g) (%)	(g) (%)	(g) (%)	(g) (%)
					Dev	Dev	Dev	Dev	Dev	Dev
					Max	Max	Max	Max	Max	Max

Load (lb)	Ht. (ft.)	4A Plate - Long Axis Vertical			4A Plate - Long Axis Horizontal			Shelf-Mounting Plate																																																																																																																																																																																																																																																																																																																																																																																																																																																															
		Direction of Blow			Direction of Blow			Direction of Blow																																																																																																																																																																																																																																																																																																																																																																																																																																																															
		Back	Edge	Top	Back	Edge	Top	Back	Edge	Top																																																																																																																																																																																																																																																																																																																																																																																																																																																													
Avg Accel Dev	Avg Accel Dev	Avg Accel Dev	Avg Accel Dev	Avg Accel Dev	Avg Accel Dev	Avg Accel Dev	Avg Accel Dev	Avg Accel Dev	Avg Accel Dev	Avg Accel Dev	Avg Accel Dev	Avg Accel Dev	Avg Accel Dev	Avg Accel Dev	Avg Accel Dev	Avg Accel Dev	Avg Accel Dev	Avg Accel Dev	Avg Accel Dev	Avg Accel Dev	Avg Accel Dev	Avg Accel Dev	Avg Accel Dev	Avg Accel Dev	Avg Accel Dev	Avg Accel Dev	Avg Accel Dev	Avg Accel Dev	Avg Accel Dev	Avg Accel Dev	Avg Accel Dev	Avg Accel Dev	Avg Accel Dev	Avg Accel Dev	Avg Accel Dev	Avg Accel Dev	Avg Accel Dev	Avg Accel Dev	Avg Accel Dev	Avg Accel Dev	Avg Accel Dev	Avg Accel Dev	Avg Accel Dev	Avg Accel Dev	Avg Accel Dev	Avg Accel Dev	Avg Accel Dev	Avg Accel Dev	Avg Accel Dev	Avg Accel Dev	Avg Accel Dev	Avg Accel Dev	Avg Accel Dev	Avg Accel Dev	Avg Accel Dev	Avg Accel Dev	Avg Accel Dev	Avg Accel Dev	Avg Accel Dev	Avg Accel Dev	Avg Accel Dev	Avg Accel Dev	Avg Accel Dev	Avg Accel Dev	Avg Accel Dev	Avg Accel Dev	Avg Accel Dev	Avg Accel Dev	Avg Accel Dev	Avg Accel Dev	Avg Accel Dev	Avg Accel Dev	Avg Accel Dev	Avg Accel Dev	Avg Accel Dev	Avg Accel Dev	Avg Accel Dev	Avg Accel Dev	Avg Accel Dev	Avg Accel Dev	Avg Accel Dev	Avg Accel Dev	Avg Accel Dev	Avg Accel Dev	Avg Accel Dev	Avg Accel Dev	Avg Accel Dev	Avg Accel Dev	Avg Accel Dev	Avg Accel Dev	Avg Accel Dev	Avg Accel Dev	Avg Accel Dev	Avg Accel Dev	Avg Accel Dev	Avg Accel Dev	Avg Accel Dev	Avg Accel Dev	Avg Accel Dev	Avg Accel Dev	Avg Accel Dev	Avg Accel Dev	Avg Accel Dev	Avg Accel Dev	Avg Accel Dev	Avg Accel Dev	Avg Accel Dev	Avg Accel Dev	Avg Accel Dev	Avg Accel Dev	Avg Accel Dev	Avg Accel Dev	Avg Accel Dev	Avg Accel Dev	Avg Accel Dev	Avg Accel Dev	Avg Accel Dev	Avg Accel Dev	Avg Accel Dev	Avg Accel Dev	Avg Accel Dev	Avg Accel Dev	Avg Accel Dev	Avg Accel Dev	Avg Accel Dev	Avg Accel Dev	Avg Accel Dev	Avg Accel Dev	Avg Accel Dev	Avg Accel Dev	Avg Accel Dev	Avg Accel Dev	Avg Accel Dev	Avg Accel Dev	Avg Accel Dev	Avg Accel Dev	Avg Accel Dev	Avg Accel Dev	Avg Accel Dev	Avg Accel Dev	Avg Accel Dev	Avg Accel Dev	Avg Accel Dev	Avg Accel Dev	Avg Accel Dev	Avg Accel Dev	Avg Accel Dev	Avg Accel Dev	Avg Accel Dev	Avg Accel Dev	Avg Accel Dev	Avg Accel Dev	Avg Accel Dev	Avg Accel Dev	Avg Accel Dev	Avg Accel Dev	Avg Accel Dev	Avg Accel Dev	Avg Accel Dev	Avg Accel Dev	Avg Accel Dev	Avg Accel Dev	Avg Accel Dev	Avg Accel Dev	Avg Accel Dev	Avg Accel Dev	Avg Accel Dev	Avg Accel Dev	Avg Accel Dev	Avg Accel Dev	Avg Accel Dev	Avg Accel Dev	Avg Accel Dev	Avg Accel Dev	Avg Accel Dev	Avg Accel Dev	Avg Accel Dev	Avg Accel Dev	Avg Accel Dev	Avg Accel Dev	Avg Accel Dev	Avg Accel Dev	Avg Accel Dev	Avg Accel Dev	Avg Accel Dev	Avg Accel Dev	Avg Accel Dev	Avg Accel Dev	Avg Accel Dev	Avg Accel Dev	Avg Accel Dev	Avg Accel Dev	Avg Accel Dev	Avg Accel Dev	Avg Accel Dev	Avg Accel Dev	Avg Accel Dev	Avg Accel Dev	Avg Accel Dev	Avg Accel Dev	Avg Accel Dev	Avg Accel Dev	Avg Accel Dev	Avg Accel Dev	Avg Accel Dev	Avg Accel Dev	Avg Accel Dev	Avg Accel Dev	Avg Accel Dev	Avg Accel Dev	Avg Accel Dev	Avg Accel Dev	Avg Accel Dev	Avg Accel Dev	Avg Accel Dev	Avg Accel Dev	Avg Accel Dev	Avg Accel Dev	Avg Accel Dev	Avg Accel Dev	Avg Accel Dev	Avg Accel Dev	Avg Accel Dev	Avg Accel Dev	Avg Accel Dev	Avg Accel Dev	Avg Accel Dev	Avg Accel Dev	Avg Accel Dev	Avg Accel Dev	Avg Accel Dev	Avg Accel Dev	Avg Accel Dev	Avg Accel Dev	Avg Accel Dev	Avg Accel Dev	Avg Accel Dev	Avg Accel Dev	Avg Accel Dev	Avg Accel Dev	Avg Accel Dev	Avg Accel Dev	Avg Accel Dev	Avg Accel Dev	Avg Accel Dev	Avg Accel Dev	Avg Accel Dev	Avg Accel Dev	Avg Accel Dev	Avg Accel Dev	Avg Accel Dev	Avg Accel Dev	Avg Accel Dev	Avg Accel Dev	Avg Accel Dev	Avg Accel Dev	Avg Accel Dev	Avg Accel Dev	Avg Accel Dev	Avg Accel Dev	Avg Accel Dev	Avg Accel Dev	Avg Accel Dev	Avg Accel Dev	Avg Accel Dev	Avg Accel Dev	Avg Accel Dev	Avg Accel Dev	Avg Accel Dev	Avg Accel Dev	Avg Accel Dev	Avg Accel Dev	Avg Accel Dev	Avg Accel Dev	Avg Accel Dev	Avg Accel Dev	Avg Accel Dev	Avg Accel Dev	Avg Accel Dev	Avg Accel Dev	Avg Accel Dev	Avg Accel Dev	Avg Accel Dev	Avg Accel Dev	Avg Accel Dev	Avg Accel Dev	Avg Accel Dev	Avg Accel Dev	Avg Accel Dev	Avg Accel Dev	Avg Accel Dev	Avg Accel Dev	Avg Accel Dev	Avg Accel Dev	Avg Accel Dev	Avg Accel Dev	Avg Accel Dev	Avg Accel Dev	Avg Accel Dev	Avg Accel Dev	Avg Accel Dev	Avg Accel Dev	Avg Accel Dev	Avg Accel Dev	Avg Accel Dev	Avg Accel Dev	Avg Accel Dev	Avg Accel Dev	Avg Accel Dev	Avg Accel Dev	Avg Accel Dev	Avg Accel Dev	Avg Accel Dev	Avg Accel Dev	Avg Accel Dev	Avg Accel Dev	Avg Accel Dev	Avg Accel Dev	Avg Accel Dev	Avg Accel Dev	Avg Accel Dev	Avg Accel Dev	Avg Accel Dev	Avg Accel Dev	Avg Accel Dev	Avg Accel Dev	Avg Accel Dev	Avg Accel Dev	Avg Accel Dev	Avg Accel Dev	Avg Accel Dev	Avg Accel Dev	Avg Accel Dev	Avg Accel Dev	Avg Accel Dev	Avg Accel Dev	Avg Accel Dev	Avg Accel Dev	Avg Accel Dev	Avg Accel Dev	Avg Accel Dev	Avg Accel Dev	Avg Accel Dev	Avg Accel Dev	Avg Accel Dev	Avg Accel Dev	Avg Accel Dev	Avg Accel Dev	Avg Accel Dev	Avg Accel Dev	Avg Accel Dev	Avg Accel Dev	Avg Accel Dev	Avg Accel Dev	Avg Accel Dev	Avg Accel Dev	Avg Accel Dev	Avg Accel Dev	Avg Accel Dev	Avg Accel Dev	Avg Accel Dev	Avg Accel Dev	Avg Accel Dev	Avg Accel Dev	Avg Accel Dev	Avg Accel Dev	Avg Accel Dev	Avg Accel Dev	Avg Accel Dev	Avg Accel Dev	Avg Accel Dev	Avg Accel Dev	Avg Accel Dev	Avg Accel Dev	Avg Accel Dev	Avg Accel Dev	Avg Accel Dev	Avg Accel Dev	Avg Accel Dev	Avg Accel Dev	Avg Accel Dev	Avg Accel Dev	Avg Accel Dev	Avg Accel Dev	Avg Accel Dev	Avg Accel Dev	Avg Accel Dev	Avg Accel Dev	Avg Accel Dev	Avg Accel Dev	Avg Accel Dev	Avg Accel Dev	Avg Accel Dev	Avg Accel Dev	Avg Accel Dev	Avg Accel Dev	Avg Accel Dev	Avg Accel Dev	Avg Accel Dev	Avg Accel Dev	Avg Accel Dev	Avg Accel Dev	Avg Accel Dev	Avg Accel Dev	Avg Accel Dev	Avg Accel Dev	Avg Accel Dev	Avg Accel Dev	Avg Accel Dev	Avg Accel Dev	Avg Accel Dev	Avg Accel Dev	Avg Accel Dev	Avg Accel Dev	Avg Accel Dev	Avg Accel Dev	Avg Accel Dev	Avg Accel Dev	Avg Accel Dev	Avg Accel Dev	Avg Accel Dev	Avg Accel Dev	Avg Accel Dev	Avg Accel Dev	Avg Accel Dev	Avg Accel Dev	Avg Accel Dev	Avg Accel Dev	Avg Accel Dev	Avg Accel Dev	Avg Accel Dev	Avg Accel Dev	Avg Accel Dev	Avg Accel Dev	Avg Accel Dev	Avg Accel Dev	Avg Accel Dev	Avg Accel Dev	Avg Accel Dev	Avg Accel Dev	Avg Accel Dev	Avg Accel Dev	Avg Accel Dev	Avg Accel Dev	Avg Accel Dev	Avg Accel Dev	Avg Accel Dev	Avg Accel Dev	Avg Accel Dev	Avg Accel Dev	Avg Accel Dev	Avg Accel Dev	Avg Accel Dev	Avg Accel Dev	A

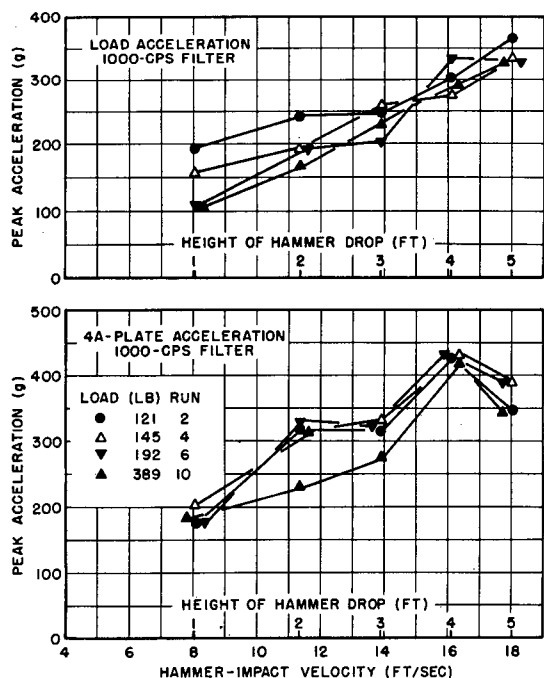


Figure 16 - Peak load and 4A-plate acceleration for edge blows, load axis horizontal

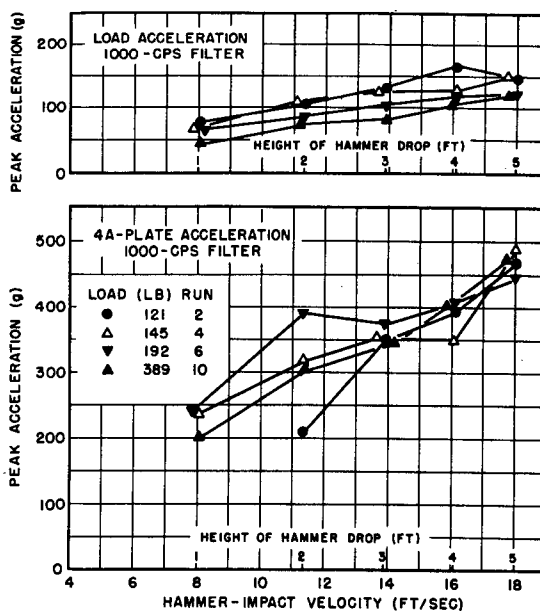


Figure 17 - Peak load and 4A-plate acceleration for top blows, load axis horizontal

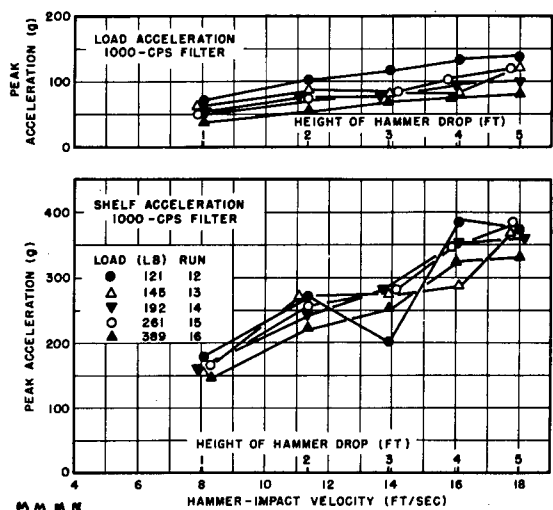


Figure 18 - Peak load and shelf-plate acceleration for back blows

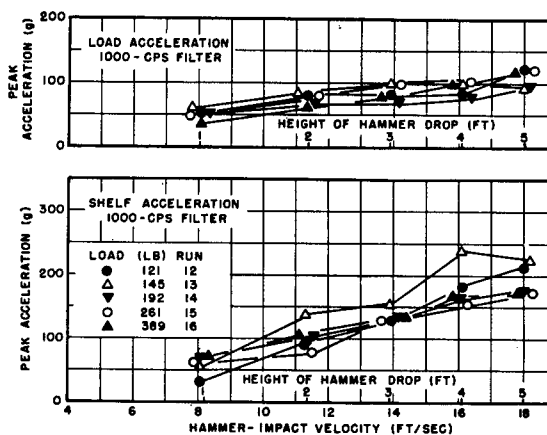


Figure 19 - Peak load and shelf-plate acceleration for edge blows

TABLE 6
Comparison of Peak Mounting-Plate Accelerations

Load (lb)	4A Plate - Long Axis Vertical			4A Plate - Long Axis Horizontal			Shelf-Mounting Plate		
	Direction of Blow			Direction of Blow			Direction of Blow		
	Back	Edge	Top	Back	Edge	Top	Back	Edge	Top
121	0.46	0.38	0.42	0.93	0.52	0.41	0.46	0.30	0.18
145	0.40	0.52	0.44	0.76	0.55	0.58	0.44	0.25	0.16
192	0.50	0.45	0.58	-	0.54	0.62	0.46	0.21	0.31
261	0.42	0.58	0.57	-	-	-	0.47	0.18	0.41
389	0.58	0.60	0.52	1.00	0.47	0.56	0.41	0.21	0.28
Avg	0.47	0.51	0.51	0.90	0.52	0.54	0.45	0.23	0.27
Group Avg	0.50			0.65			0.32		

the smallest. Edge and top blows (for any one arrangement) were approximately equivalent as would be expected from the plate symmetry for these blows. They caused less acceleration than back blows on the shelf plate and 4A plate with horizontally mounted loads.

Plots of the peak plate accelerations obtained with the 1000-cps filter are included on Figures 12 to 20 along with the corresponding peak load accelerations. Values up to 840 g were recorded at the accelerometer position (1000-cps filter) for a 5-ft blow, with the majority of values for different test conditions being in the neighborhood of 500 g.

Load Velocity

Waveforms of velocity measured on the load (\dot{x}_L) are shown as the upper trace of the typical test records (Figures 10 and 11). Two basic types of waveforms were obtained for the majority of test conditions: a damped (1-cos) function wherein the velocity built up to a peak value in a sinusoidal manner, followed by the damped low-frequency periodic vibration of the rigid-body motion; or an impulsive step-type of velocity change which reached its peak velocity relatively quickly, accompanied by small amplitude rigid-body motions. Velocity waveforms of the first type were produced on the 4A plate for back and edge blows delivered to the instrument load (Run 0) and vertically oriented rigid loads, while the second type appeared for top blows delivered to the above conditions and to all horizontally oriented loads on the 4A plate regardless of the direction of blow. In many cases it is difficult to positively identify a particular test condition as belonging to one group to the exclusion of the other. The impulsive type of velocity change represents the most inflexible type of mounting condition and would be expected for types of mounting or directions of hammer impact where the stiffness of the supporting members is great, as the test results indicate. Rigid loads with the long axis vertical (short dimension spanning the 4A plate) bind the 4A plate far less than horizontally positioned equivalent loads, and, consequently, are afforded more flexibility in their attachment for back and edge blows. This advantage is somewhat neutralized for top blows since the most rigid axes of load and 4A plate are aligned in this direction.

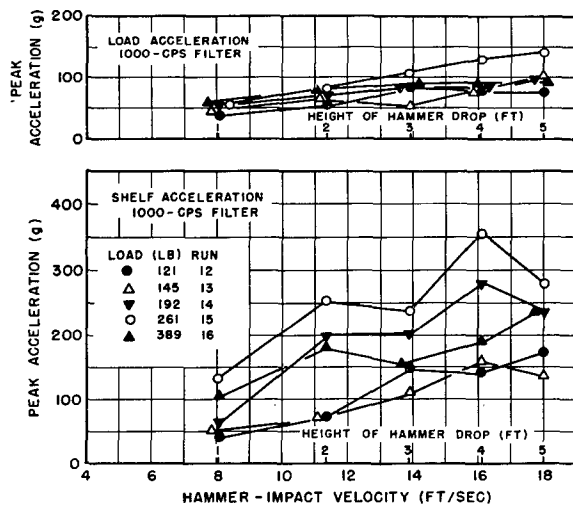


Figure 20 - Peak load and shelf-plate acceleration for top blows

Velocity waveforms recorded on the shelf mounting plate are similar in overall characteristics to those exhibited on the 4A plate, except that the line of demarcation between types of waveform is less distinct and frequencies of vibration are generally lower. These velocity waveforms are further complicated by the fact that, with the shelf-mounting arrangements, the system is no longer an approximate single-degree-of-freedom system. Since the hammer impact is directed along a line which does not contain the center of mass, a rotational component is coupled to the translational mode, and the motion then becomes a function of both. Although the pickups are sensitive to only translatory motions perpendicular to their bases, the waveforms contain components resulting from the rotational degrees of freedom due to the coupling which exists between modes, and are in general more difficult and complex to analyze.

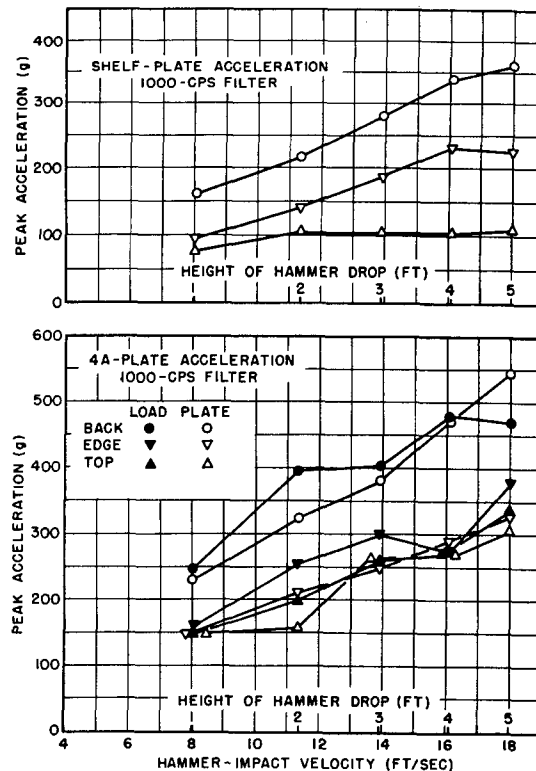


Figure 21 - Peak 4A- and shelf-plate acceleration for instrument load only

Velocity records are less sensitive to high-frequency components in the load motion than are acceleration records, and, consequently, show the lower rigid-body frequencies to better advantage. Predominant load frequencies, sustained long enough to permit evaluation, are listed in Table 7 and plotted against load weight in Figure 22. Fundamental frequencies on 4A-plate loads ranged between 194 and 88 cps, and between 81 and 41 cps for shelf-mounted loads; both arrangements showed a tendency to decrease in frequency with an increase in load weight. Higher frequency modes, which appear to be harmonically related to the fundamental, were sometimes excited and were predominant on acceleration records. The correspondence between natural frequencies and peak acceleration which might be expected from vibrational theory is suggested by a comparison of Tables 3 and 7, although some levels are not in the correct ratio. Loads mounted with their long axes horizontal on the 4A plate indicate higher frequencies and greater peak accelerations than corresponding loads vertically oriented for back and edge blows, while the reverse is true for top blows. Natural frequencies and peak accelerations are less on shelf-mounted loads than on any arrangement on the 4A plate.

TABLE 7
Predominant Load Frequencies
(Cycles per Second)

Load (lb)	4A Plate - Long Axis Vertical			4A Plate - Long Axis Horizontal			Shelf-Mounting Plate		
	Back	Edge	Top	Back	Edge	Top	Back	Edge	Top
57	114	174	148				-	127	61
121	128	182	160	167/334	188	121	42/247	70	51
145	120	168	137	165/333	189	120	47/231	81	220
192	115	162	138	155/314	194	105	42/223	79	204
261	97	147	-	-	-	-	48/213	78	58/183
389	88	138	-	96	154	-	41	77	67

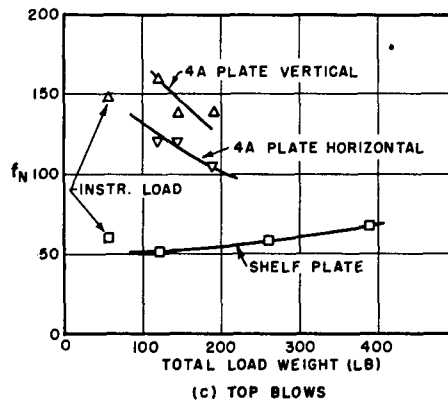
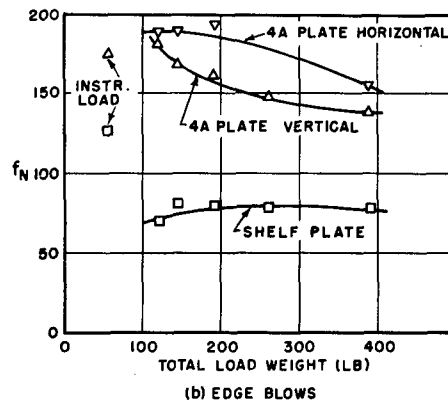
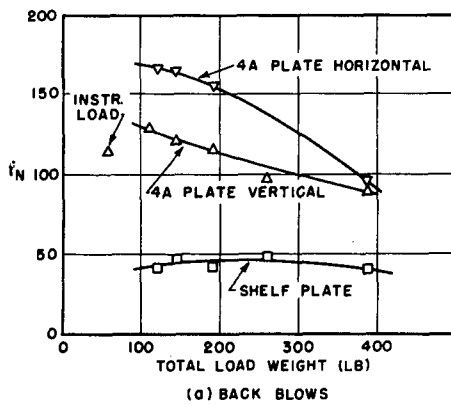


Figure 22 - Predominant load frequencies

The maximum load velocities attained for each test arrangement are plotted against hammer-impact velocity as Figures 23 through 31. On the average, these plots indicate a linear relationship to the hammer momentum except at the higher hammer drops (especially for edge blows) where the decreasing slope of the curves indicates energy absorption through plastic deformation in the struck members. Table 8, based on the average slopes of the peak load-to-hammer velocity-transfer characteristic and adjusted to a per-unit basis, was constructed to assist in comparison of peak-velocity values for the different conditions of test. Loads mounted on the 4A plate yielded peak velocities which were greatest for edge blows and least for top blows. Little difference resulted between values obtained for corresponding directions of hammer blow due to changes of load orientation. Peak velocities measured on shelf-mounted loads were less than those on the 4A plate. Peak load velocities in the neighborhood of 15 ft/sec were recorded for a 5-ft back hammer drop during one of the lighter-load runs using the 4A plate; this value reduced to about 10 ft/sec as the load was increased to 389-lb.

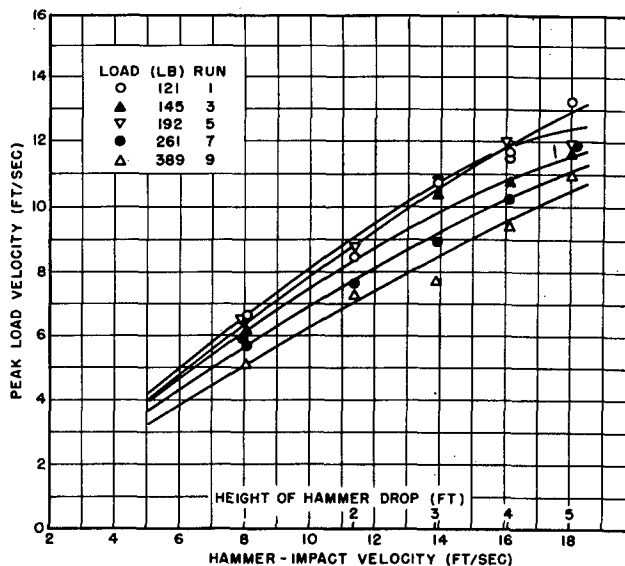


Figure 23 - Peak load velocity for back blows on 4A plate, load axis vertical

TABLE 8
Comparison of Peak Velocities

Load (lb)	4A Plate - Long Axis Vertical			4A Plate - Long Axis Horizontal			Shelf-Mounting Plate		
	Back	Edge	Top	Back	Edge	Top	Back	Edge	Top
57	0.88	0.94	0.62				0.52	0.69	0.46
121	0.76	0.84	0.58	0.73	0.84	0.69	0.59	0.55	0.38
145	0.72	1.00	0.50	0.71	0.75	0.62	0.61	0.52	0.34
192	0.76	0.97	0.44	0.66	0.66	0.53	0.65	0.51	0.36
261	0.69	0.74	0.47	-	-	-	0.55	0.48	0.35
389	0.61	0.70	0.40	0.58	0.56	0.40	0.52	0.39	0.36
Avg	0.71	0.85	0.48	0.67	0.70	0.56	0.58	0.49	0.36
Group Avg	0.68			0.64			0.48		

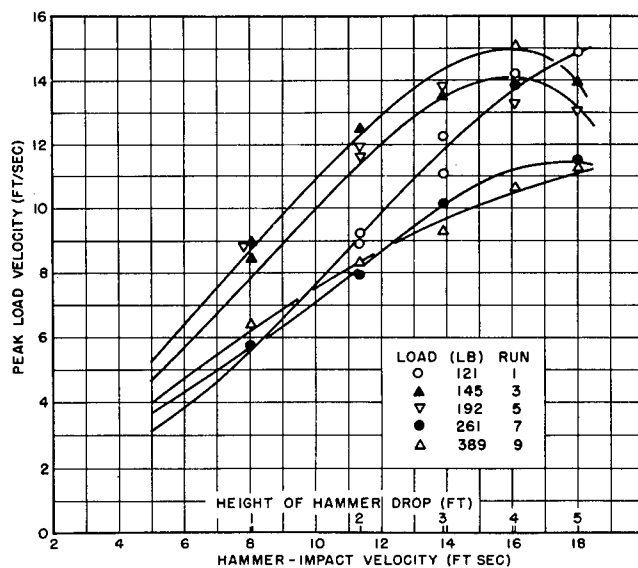


Figure 24 - Peak load velocity for edge blows on 4A plate, load axis vertical

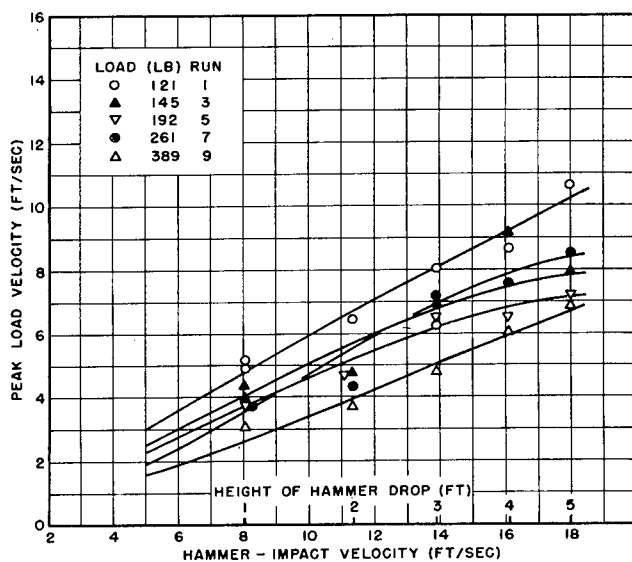


Figure 25 - Peak load velocity for top blows on 4A plate, load axis vertical

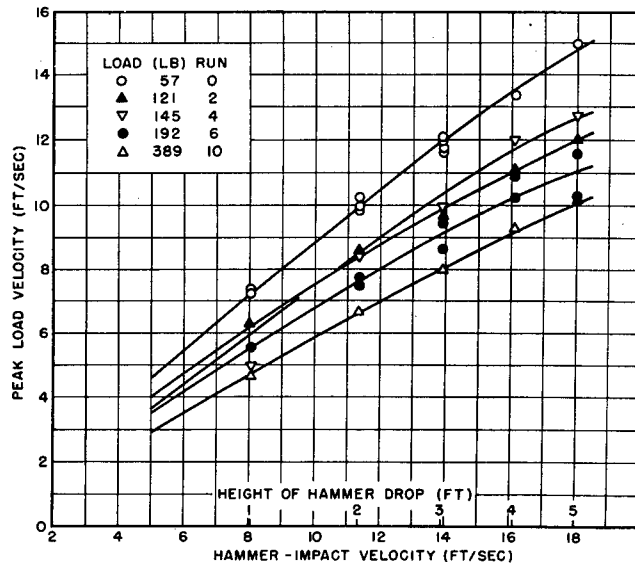


Figure 26 - Peak load velocity for back blows on 4A plate, load axis horizontal

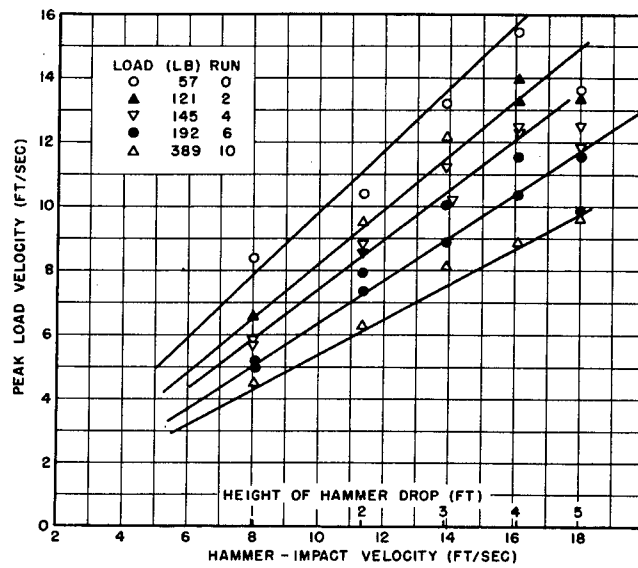


Figure 27 - Peak load velocity for edge blows on 4A plate, load axis horizontal

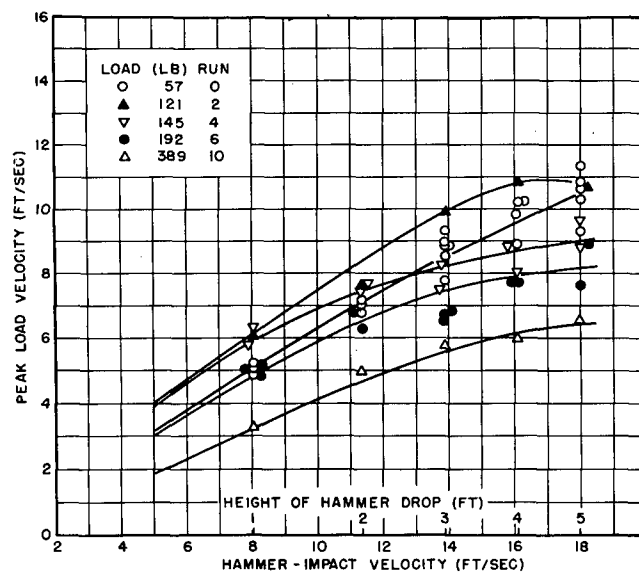


Figure 28 - Peak load velocity for top blows on 4A plate, load axis horizontal

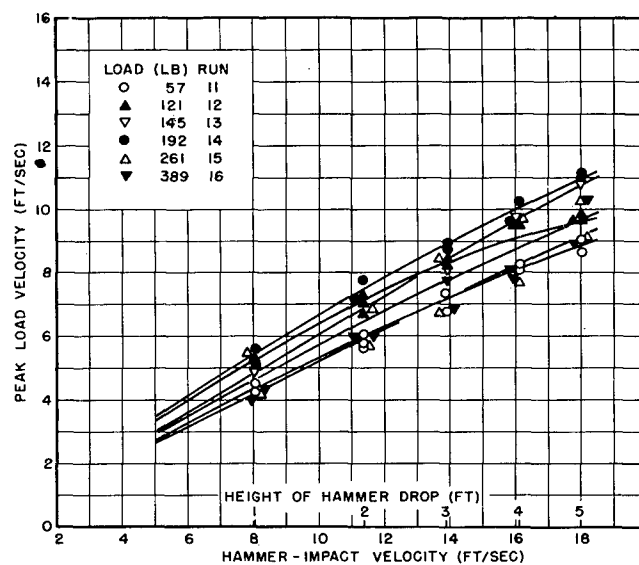


Figure 29 - Peak load velocity for back blows on shelf-mounting plate

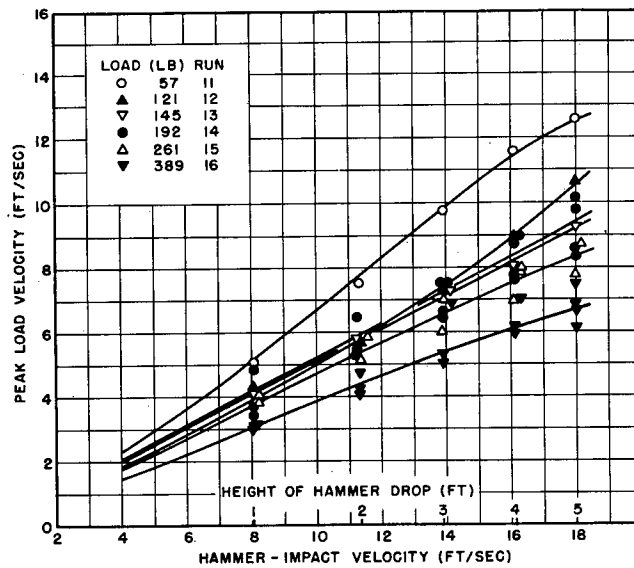


Figure 30 - Peak load velocity for edge blows on shelf-mounting plate

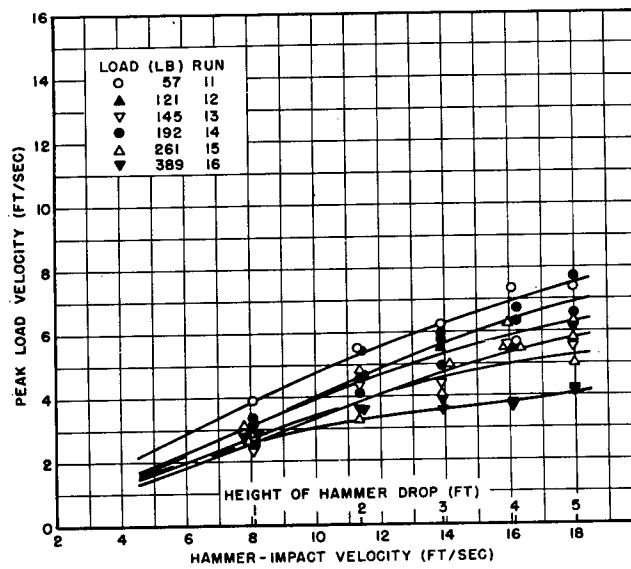


Figure 31 - Peak load velocity for top blows on shelf-mounting plate

Load Displacement

Load displacement-time curves (Figures 32 and 33) were computed for a few representative test conditions by graphically integrating load-velocity records. Although this method becomes increasingly less accurate as the integration period is extended, the low natural frequency (2.5 cps) of the modified MB velocity meters permitted the evaluation to be carried out to the peak displacement without appreciable error. During 5-ft hammer drops, the time to peak displacement varied from about 20 milliseconds, for the 4A mounting plate unloaded, to about 40 milliseconds for a maximum load of 389 lb.

The plots indicate several interesting attributes of the displacement characteristics of the light weight machine. When the 4A plate is lightly loaded, as with the instrument load, the fundamental displacement motions imparted by the different directions of hammer blow are nearly identical. The increased flexibility of the 4A plate for back blows is evidenced by the oscillatory component of its displacement curve, although its center of mass displacement (average displacement disregarding the periodic variations) closely approximates that obtained for edge and top blows. Addition of a 389-lb rigid load produces pronounced changes in the displacement characteristics between directions, in addition to increasing the time to peak displacement. Back-blow displacements get under way faster than either edge or top blows, although they may not experience the allowable 1.5-inch travel at the load position, owing to the phasing of the vibrational component. Edgeblows start more slowly but reach a higher peak displacement in a comparable

interval, suggesting a lower initial, but more consistent, velocity. Displacements resulting from top blows are the slowest in reaching their peak. Load orientation is relatively unimportant with regard to displacement amplitudes or time to the peak.

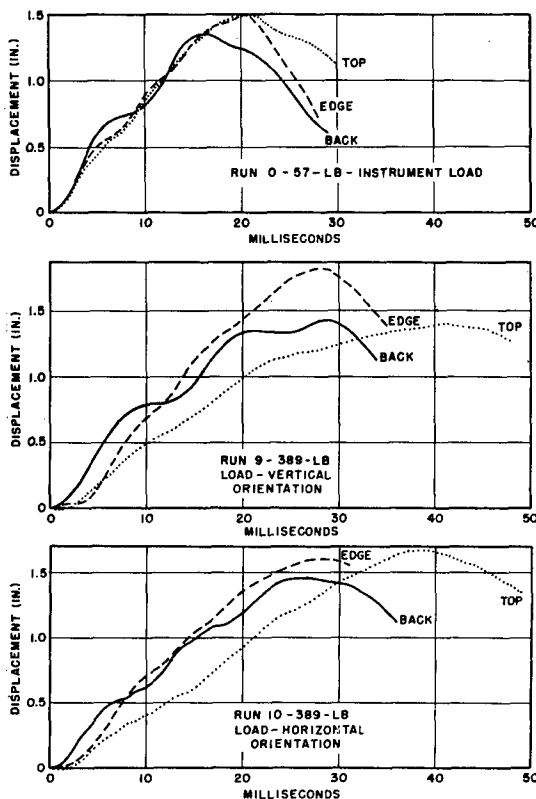


Figure 32 - Displacement-time curves plotted from integrated velocity records for 5-ft hammer drops on the 4A-mounting plate

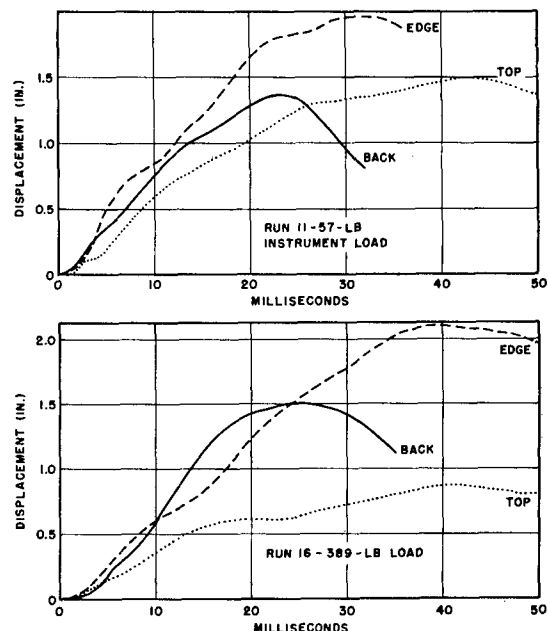


Figure 33 - Displacement-time curves plotted from integrated velocity records for 5-ft hammer drops on the shelf-mounting plate

Displacement-time curves for shelf-mounted loads are quite different from similar loads on the 4A plate. Differences manifest themselves mainly in the large variations between directions of hammer impact even for light loads, and in insignificant changes in time to the peak value with large increases in load weight. The initial slopes of the displacement-time curves for shelf-mounted loads are nearly identical up to about 4 milliseconds, after which the curves diverge.

Several instances are evident, particularly during edge blows, where the integrated velocity yielded a peak displacement in excess of the preset limit value of 1.5 inches. In one event it obtained 2.1 inches. These extreme excursions are accounted for by the flexibility of the machine framework responsible for stopping the anvil at the end of its permissible travel and the phasing of the local vibrations of the load.

Reproducibility of Data

As the test progressed, it became more evident that the measurements were being influenced to a noticeable extent by uncontrolled machine parameters which depended largely on previous history. Prior to this investigation, the anvil plate had seen considerable service during routine shock tests and was deformed in a manner common to all anvil plates after a moderate number of blows, i.e., the plate was bowed slightly from backblows, and all shock-pads were indented to the shape of the spherical hammers; nevertheless, all welds were tight. Common practice dictates that these plates are considered satisfactory for shock tests until the deformations become excessive (above one-inch separation due to deformation of the center of the anvil plate from a chord extended from its edges) or until weld failures occur. The condition of this anvil plate was probably equivalent to the majority of those in operation on other machines and might be termed average. Both the 4A and shelf mounting plates were in new condition at the outset, having only the holes required to secure the loads and instruments in their various locations. Ordinarily these plates are used until the holes become too numerous to permit drilling additional holes, after which the plates are discarded.

The test agenda was arranged to conform to the easiest transition from one test condition to the next, except that blows from all three directions were delivered before passing on to the next condition. By choice, the no-load run was made first on the 4A plate, followed by increasingly heavier rigid loads. At the conclusion of testing, a duplicate set of data again was taken under no-load conditions. The results of top blows are representative and

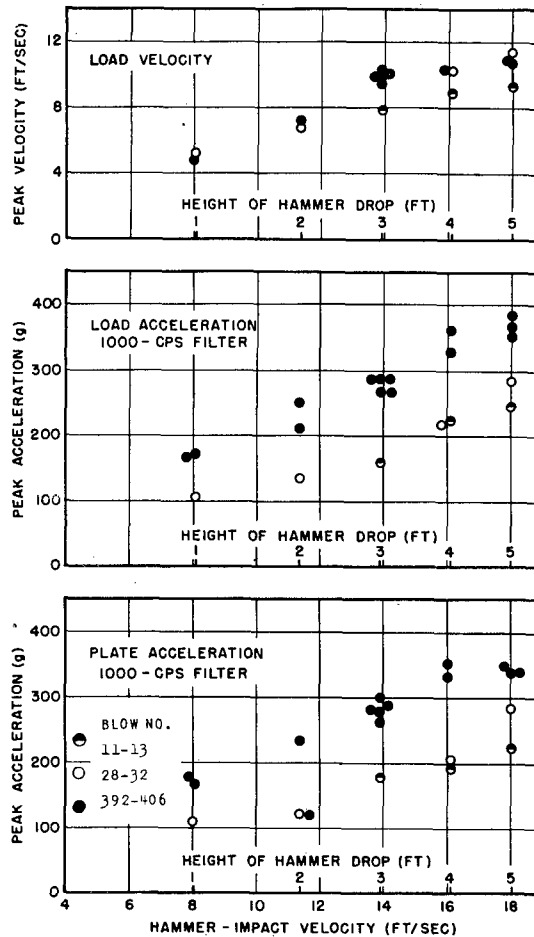


Figure 34 - Peakload and 4A-plate acceleration obtained by repeated top blows, 57-lb instrument load

are plotted in Figure 34. Peak load and 4A-plate accelerations were approximately the same in this instance, since the instruments comprised the only load on the 4A plate and thus did not restrict the plate's motion. Peak accelerations measured during the first series, blows 11-13 and 28-32, show a small amount of scatter and an approximate linear relationship with hammer-impact velocity. Likewise, data taken during blows 392-406 evidence a local consistency of peak values, yet the general level of the latter experimental data ran almost 60 percent higher. Peak velocities evidenced the same general trends with minor variations, although the scatter was not as pronounced, as might well be expected for a lower-order function. Differences between these values can most likely be attributed to changes in stiffness of the anvil assembly as a result of work hardening and pad deformation. The spread in damage potential for practical equipment would be more similar to that shown by the velocity measurements rather than by the acceleration measurements, because damage more generally results from the lower-frequency component of shock motions.

SUMMARY

The light weight shock machine has been used extensively during the past decade for improving the shock resistance of naval shipboard equipment. Shock motions imparted to the anvil plate are essentially impulsive in character; that is, they constitute a very large force acting for a short time, usually about one millisecond, and are intended to duplicate the type of motions experienced by a ship's hull as the result of a nearby, noncontact underwater explosion. Equipment to be shock tested is not mounted directly on the anvil plate, but is bolted to an auxiliary mounting plate, which affords it a degree of flexibility comparable to that possessed by the decks and bulkheads in the internal sections of the ship. The energy stored in deforming these structures greatly alters the wave shapes and amplitudes of the initial shock motions imparted to the anvil plate, and reduces the initial acceleration by extending the time over which the velocity change occurs. Much of this energy is subsequently released as damped oscillatory motions occurring at the natural frequency of the load and mounting-plate system. Because of the sharp wavefronts present in the shock wave and because of the coupling which exists between modes of vibration in the mounting plate, numerous other nonperiodic high-frequency motions are present, which are more pronounced in acceleration records.

The shock motions resulting from blows delivered from the back, edge, and top vary considerably for identical hammer energies. The 4A-plate stiffness is greater from edgewise directions than it is from the back, although these differences are mitigated to a considerable extent by the increased load-moment arm when struck from either the edge or top. The physical size and stiffness of the test equipment also has a bearing on the accelerations imposed. Stiff frames and housings bind the mounting plate in the area covered by the base dimensions, making it stiffer, and consequently subjecting internal parts of the equipment to greater peak accelerations. On the other hand, less-stiff frames flex with the mounting plate and expose their component parts to misalignment and interference, although the peak accelerations are somewhat attenuated. In addition, the span of the mounting dimensions is important in determining peak forces on the equipment, since the points of support move into areas of increasing acceleration magnitudes as they approach the spacer channels. Acceleration magnitudes on the shelf-mounting adaptors would be expected to be less than those on the 4A plate, owing to the additional structure through which the shock must pass and because of the extra flexibility afforded by this configuration.

Measurements made during the course of this investigation bear out the principal features of the above remarks. A maximum value of 537 g (1000-cps filter) was measured on the load when horizontally oriented on the 4A plate and subjected to a 5-ft back blow. The same load experienced a peak acceleration in the neighborhood of 200 g when vertically oriented on the 4A plate, and only 121 g when mounted on the shelf mounting

plate. These values are applicable only to loads which approximate the size and rigidity of the test loads, and depend to some extent on the tightness of the bolted connections and the general condition of the mounting and anvil plates.

Peak-acceleration values given in this report are generally lower than have been reported in the past. There are two reasons for this: first, older instrumentation techniques employed 12,000- or 5,000-cps filters permitting the high-frequency components to dominate the record; and second, measurements were often taken directly over the spacer channels on the 4A plate. The peak values reported herein were obtained directly on the load, and contained only those components whose frequencies were low enough to excite damaging natural frequencies in practical systems.

CONCLUSIONS

The following conclusions result from this study:

1. The magnitude and nature of the shock motions resulting from blows delivered to the back, edge, or top of the anvil plate vary considerably for identical hammer-impacting velocities. This variation is inherent for an anvil of this general design and for the mounting methods employed. While it is possible that improvements can be made to provide more uniformity of shock, equivalent values for the three directions cannot be obtained.

2. A short practical study of the shock-machine characteristics can be done by means of a velocity pickup of the seismic type. The pickup should have a natural frequency of about 2 cps and be capable of measuring to 1000 cps. Minimum pickup coil displacements up to 3 inches relative to the instrument case should be available. Analysis, for comparison purposes, can be done most simply by peak values. A later report will concern itself with reed gages and shock-spectra methods of measurement and analysis.

3. The intensity of the high-frequency components of shock motions increases with the amount of use of the anvil assembly. This is probably caused by work hardening and an establishment of residual stresses in the assembly. The intensity change is not as great when measured by a velocity pickup, which does not accentuate the higher frequencies, as when measured in terms of acceleration. It is probable that the causes of the major differences in performances of different machines of this type result from nonuniformity of anvil-assembly material, heat treatment, and previous use. It would be preferable to have the anvil assembly designed in such a manner that plastic deformation does not occur. This is done in the case of the medium weight machine and the shock machine for electronic devices.

4. The acceleration magnitudes reported at this time are less than previously reported because of lower cutoff values used for filtration (1000 cps rather than 5000 and 12,000 cps) and because the accelerations were measured on the load or on the mounting panel distant from the spacer channels.

5. For a given load and mounting arrangement, and for only elastic deformations and tightly bolted connections, it would be expected that the maximum values of acceleration and velocity would be linearly proportional to the hammer-impact velocity. This assumes that the hammer-anvil contact time is independent of impact velocity. The data points plotted for acceleration have been connected by straight lines because of unpredictable fluctuations caused by minor variations in bolt tightness and load assembly. The maximum accelerations measured on the mounting plate are quite independent of the load. The accelerations of the load, however, decrease with increasing load magnitude. The maximum velocities more nearly follow the linear

relation with hammer-impact velocity, except for the highest drops where plastic deformation can be expected. The variation of maximum velocity with load follows in inverse proportion to the change in total weight of the load-anvil assembly.

ACKNOWLEDGMENTS

The task of compiling the experimental data for this report was performed as a joint effort by personnel of the Structures Branch and the Shock and Vibration Branch of the Mechanics Division. In particular, acknowledgment is due J. L. Bachman, J. W. Whyte, A. F. Dick, and R. C. Cowan for handling the mechanical details of the test; R. Q. Tillman for operating the recording equipment; and R. J. Peters for assisting in analysis of the recorded data.

* * *

REFERENCES

- (1) Conrad, R. W., "Characteristics of the 250 Ft-Lb Shock Machine," NRL Report F-3328, July 22, 1948
- (2) Norgorden, O., and Shanahan, F. J., "A Device for Mechanical Test of Electronic Equipment," Shock and Vibration Bulletin No. 3, p. 43; NRL Report S-3106, May 1947
- (3) Kirkpatrick, T. P., "Medium Weight High-Impact Shock Machine Characteristics," Symposium on Shock, Vol. II, p. 48, BuShips, Oct. 30, 1943
- (4) Conrad, R. W., "Characteristics of the Medium Weight Shock Machine," NRL Report 3852, Sept. 14, 1951
- (5) Vigness, I., "Mechanical Shock Characteristics of the Armor High-Impact Machine for Electronic Devices (Armour Research Foundation Machine # 1)," NRL Report O-2485, March 1945
Vigness, I., Kammer, E. W., and Holt, S., "Mechanical Shock Characteristics of the High-Impact Machine for Electronic Devices (NRL Machine #1)," NRL Report O-2497, March 1945
Vigness, I., Nowak, R. C., and Kammer, E. W., "Mechanical Shock Characteristics of High-Impact Machines for Electronic Devices," (Taft-Pierce Manufacture), NRL Report O-2838, Dec. 1946
- (6) Johnson, K. W., "Shock Machine, Medium Impact, Variable Duration," USAF, AMC Memorandum Report MCREE-49-10, Feb. 18, 1949
- (7) Conrad, R. W., "Characteristics of the 3 Ft-Lb Vibration Machine," NRL Report S-3186, Oct. 1947
- (8) Powell, H. R., "Drop-Table Type Shock Tester," Boston Univ., Upper Atmosphere Research Lab., Tech. Note No. 9, Aug. 15, 1950
- (9) Young, S. E., "Effect of Modifications on the Performance Characteristics of the Light Weight, High-Impact Shock Machine," NRL Report V-2666, Oct. 15, 1945
- (10) BuShips Specification 40T9 (SHIPS), Dec. 15, 1946
- (11) Military Specification MIL-S-901 (SHIPS), Nov. 15, 1949
- (12) Dorr, G. W. "Investigation of Characteristics of Mechanical Shock on H. I. Shock Machine," NRL ltr report 3853-323A/50 GWD:mb to BuShips, Sept. 6, 1950